

RESEARCH ARTICLE

Delineating CD4 dependency of HIV-1: Adaptation to infect low level CD4 expressing target cells widens cellular tropism but severely impacts on envelope functionality

David Beauparlant¹, Peter Rusert¹, Carsten Magnus^{1#a}, Claus Kadelka^{1,2}, Jacqueline Weber¹, Therese Uhr¹, Osvaldo Zagordi¹, Corinna Oberle^{1#b}, Maria J. Duenas-Decamp³, Paul R. Clapham³, Karin J. Metzner^{1,2}, Huldrych F. Günthard^{1,2}, Alexandra Trkola^{1*}

1 Institute of Medical Virology, University of Zurich, Zurich, Switzerland, **2** Division of Infectious Diseases and Hospital Epidemiology, University Hospital Zurich, Zurich, Switzerland, **3** Program in Molecular Medicine, Biotech II, University of Massachusetts Medical School, Worcester, Massachusetts, United States of America

#a Current address: Department of Biosystems Science and Engineering, ETH Zürich, Basel, Switzerland

#b Current address: Gilead Sciences Switzerland Sarl, Zug, Switzerland

* trkola.alexandra@virology.uzh.ch



OPEN ACCESS

Citation: Beauparlant D, Rusert P, Magnus C, Kadelka C, Weber J, Uhr T, et al. (2017) Delineating CD4 dependency of HIV-1: Adaptation to infect low level CD4 expressing target cells widens cellular tropism but severely impacts on envelope functionality. *PLoS Pathog* 13(3): e1006255. doi:10.1371/journal.ppat.1006255

Editor: David T. Evans, University of Wisconsin, UNITED STATES

Received: December 6, 2016

Accepted: February 22, 2017

Published: March 6, 2017

Copyright: © 2017 Beauparlant et al. This is an open access article distributed under the terms of the [Creative Commons Attribution License](https://creativecommons.org/licenses/by/4.0/), which permits unrestricted use, distribution, and reproduction in any medium, provided the original author and source are credited.

Data Availability Statement: All relevant data are within the paper and its Supporting Information files.

Funding: Financial support for this study was provided by the Swiss National Science Foundation. Financial support for this study has been provided by the Swiss National Science Foundation (<http://www.snf.ch>; grants 314730_152663 and 310000-135527 to AT) and the University of Zurich's Clinical Research Priority Program: Viral Infectious

Abstract

A hallmark of HIV-1 infection is the continuously declining number of the virus' predominant target cells, activated CD4⁺ T cells. With diminishing CD4⁺ T cell levels, the capacity to utilize alternate cell types and receptors, including cells that express low CD4 receptor levels such as macrophages, thus becomes crucial. To explore evolutionary paths that allow HIV-1 to acquire a wider host cell range by infecting cells with lower CD4 levels, we dissected the evolution of the envelope-CD4 interaction under *in vitro* culture conditions that mimicked the decline of CD4^{high} target cells, using a prototypic subtype B, R5-tropic strain. Adaptation to CD4^{low} targets proved to severely alter envelope functions including trimer opening as indicated by a higher affinity to CD4 and loss in shielding against neutralizing antibodies. We observed a strikingly decreased infectivity on CD4^{high} target cells, but sustained infectivity on CD4^{low} targets, including macrophages. Intriguingly, the adaptation to CD4^{low} targets altered the kinetic of the entry process, leading to rapid CD4 engagement and an extended transition time between CD4 and CCR5 binding during entry. This phenotype was also observed for certain central nervous system (CNS) derived macrophage-tropic viruses, highlighting that the functional perturbation we defined upon *in vitro* adaptation to CD4^{low} targets occurs *in vivo*. Collectively, our findings suggest that CD4^{low} adapted envelopes may exhibit severe deficiencies in entry fitness and shielding early in their evolution. Considering this, adaptation to CD4^{low} targets may preferentially occur in a sheltered and immune-privileged environment such as the CNS to allow fitness restoring compensatory mutations to occur.

Diseases (<http://www.uzh.ch/en/research/medicine/clinic.html>; to AT and HFG). The Swiss HIV Cohort Study is financed in the framework of the Swiss National Science Foundation (grant 33CS30_148 522). The funders had no role in study design, data collection and analysis, decision to publish, or preparation of the manuscript.

Competing interests: All authors including Corinna Oberle have declared that no competing interests exist. Corinna Oberle declares that the work she contributed to the current study was conducted during her PhD thesis in the group of Prof Huldrych Günthard at the University Hospital Zurich. Corinna Oberle further declares that the work is in no connection to her current appointment as a specialist for HCV at Gilead Sciences and that no competing interests exist.

Author summary

Untreated HIV-1 infection leads to a gradual depletion of CD4⁺ T cells forcing the virus to continuously adapt to an ever-decreasing number of suitable target cells. Our data based on experiments in a highly controlled *in vitro* setting describe one avenue of envelope adaptation that allows the virus to infect target cells expressing low amounts of CD4 such as macrophages. Analysis of the functional envelope phenotypes associated with adaptation of the virus to infect target cells expressing low levels of CD4 highlighted altered entry kinetics of the virus. These alterations resulted in extended exposure of CD4-induced neutralization sensitive epitopes in combination with an increased sensitivity to neutralizing antibodies targeting the CD4 binding site and the V3 loop. Interestingly, a similar phenotype was observed for macrophage-tropic HIV-1 isolates derived from the central nervous system (CNS) of infected individuals raising the possibility that the immune-privileged CNS may favor the development of macrophage-tropic / low CD4 level utilizing envelope variants.

Introduction

The infection cycle of HIV-1 is intimately linked with the CD4 receptor on target cells. Entry is initiated by the binding of the viral envelope glycoprotein gp120 to CD4, necessitating a high conservation of the CD4 binding site (CD4bs) on the viral envelope [1]. At the same time, the virus faces a humoral immune response targeting the CD4bs [1–4] and disease progression decreases the pool of available CD4 expressing target cells [5–8]. During disease progression multiple forces are therefore acting on the envelope glycoprotein and its interplay with CD4. How these factors shape envelope functional adaptation, and which combination of selective forces is responsible for giving rise to viral phenotypes observed at late disease stages remains unclear. A particular conundrum is the capacity of HIV-1 to maintain high level virus production at late disease stages, even when the classical target cells, CD4⁺ T cells, are heavily depleted [9–12]. Because of this, it was suggested for some time that HIV-1 resolves to replicate in other cell types at later stages [13, 14], which can be linked with use of alternative coreceptors (reviewed in [15–17]). Differential receptor usage most commonly includes varying the capacity of Env to bind CD4 or CCR5, and switching coreceptor use to CXCR4. All of these phenotypes have been observed in late disease states *in vivo* [18–22].

HIV-1 enters host cells by first binding to CD4 [23, 24] via the gp120 surface glycoprotein subunit [25]. CD4 binding triggers conformational changes in gp120 that expose the co-receptor binding sites to attach to either of the two main co-receptors; CCR5 (R5) [26, 27] or CXCR4 (X4) [28]. The dynamics of CD4 and CCR5 and/or CXCR4 use are important determinants of cellular tropism and transmission of HIV-1. Receptors are expressed independently in various combinations and at different levels on a multitude of human cells, rendering specific cell types differentially susceptible to specific envelope variants [22, 29, 30]. R5 tropic envelopes almost exclusively establish infection [31–34] and allow for the infection of activated effector memory CD4⁺ T cells [35], macrophages, and dendritic cells [36]. A switch in co-receptor use, from R5 to X4 tropism, is well documented at later disease stages, has been observed in 20–50% of patients [37–41] and described in non-human primates (NHP) [42, 43]. CXCR4 usage results in an expansion of cellular tropism of the virus to include naïve CD45RA⁺ CD4⁺ T-cells, which lack CCR5 expression [36], and has often been associated with disease progression [32, 44–47]. Likewise, increased replicative fitness of R5 viruses in later

stages of infection has also been linked with rapid disease progression [44, 48–54] though this is not universal [55].

During the course of infection, the HIV-1 envelope must adapt to facilitate replication despite a decrease in its preferred CD4⁺ target cell population. Acute infection rapidly depletes the activated CD4⁺ T cells expressing high CCR5 co-receptor levels abundant in the GALT (gut-associated-lymphoid-tissue) and the genital mucosa [10, 56]. In addition to the death of infected cells, the dramatic reduction in total CD4⁺ T cell counts observed in HIV-1 infection is considered mainly due to apoptotic and bystander cell death [57–60] and possibly killing of CD4⁺ T cells following abortive infection with HIV via pyroptosis [7, 12].

In the progression of untreated infection, the virus thus needs to expand its cellular tropism by gaining access to different tissue compartments and adapting to utilize suboptimal receptor levels and different receptors in humans [61, 62] and NHP models [42, 43]. This is well documented by studies on viruses derived from the central nervous system (CNS). Envelopes from virus circulating in this compartment often display elevated macrophage tropism that has mainly been attributed to an improved affinity for CD4. Paired with almost unanimous R5-usage, increased CD4 affinity allows the virus to infect macrophages expressing low levels of CD4 [20, 21, 63–68]. Macrophage tropism has also been attributed to an increased affinity for CCR5 [20, 69–71]. Consequently, at late disease stages the ability to use low levels of CD4 and R5 or X4, or dual (R5X4) tropism, can provide these envelopes with a broad cellular tropism including macrophages, T cells, DCs and even microglia [21, 36, 63, 66, 69, 72–74].

Thus, the co-evolutionary arms race between the immune system and virus, in combination with the ever-decreasing availability of target cells, produces a complex composition of possible envelope-receptor tropisms specific to disease stages and/or body compartments. Numerous studies have phenotypically characterized envelopes displaying altered receptor- and cellular- tropisms. The impressive body of previous work has almost exclusively focused on identifying associated phenotypes of, and specific mutations associated with, macrophage-tropism derived during infection *in vivo*. The envelopes used in the literature have been isolated from patient material and as such have developed *in vivo* under an undefined collection of selective forces. One of the foremost phenotypes consistently associated with macrophage tropism is the ability to use low levels of CD4. Our study explores the impact that a CD4^{low} selective force has on the resulting envelope phenotype when applied in isolation to address the question whether low CD4 availability by itself is sufficient to generate macrophage tropism.

In this study, we specifically explored the impact of a target cell environment low in available CD4 receptor numbers (CD4^{low}), as this may gain in importance at late disease stages during HIV-1 infection. Utilizing an R5 virus isolated from a chronically infected individual, we exposed it to an artificially induced CD4^{low} PBMC environment using a CD4 D1-domain binding DARPin that blocks gp120 binding to CD4 [75]. We show that adaptation of the HIV-1 envelope glycoprotein to CD4^{low} PBMC is sufficient to produce a phenotype similar to that observed in the CNS *in vivo*, displaying high sensitivity to CD4 and neutralizing antibodies as well as increased macrophage tropism. Adaptation to CD4^{low} PBMC resulted in evolution of envelope variants with a higher affinity to CD4 but decreased fitness. Envelopes with a CD4^{low} adapted phenotype suffer reduced particle infectivity, prolonged entry step transitions and increased neutralization sensitivity. We lastly extend the observation of long entry step transitions to several extensively described CNS-derived macrophage-tropic Envs [64, 76–79]. In combination these observations highlight that the emergence of CD4^{low} using viruses must overcome multiple barriers *in vivo*, likely requiring a range of compensatory mutations to offset the reduced neutralization resistance and entry capacity, providing an explanation as to why virus strains with these properties have been observed before the onset of potent neutralization responses [80] and have often been isolated from the immune-privileged CNS [66, 74, 81].

Results

Adapting HIV-1 to utilize target cells expressing low amounts of CD4

In the present study we were interested to follow the evolution of the HIV-1 envelope protein when confronted with the selective pressure of a cell environment with low CD4 receptor availability. The starting point of our analysis was a subtype B, R5-tropic virus isolate called NAB01, derived during chronic infection [82, 83]. The process of adaptation of this virus to low CD4 expressing target cells and the chronology of clones generated to form an envelope evolution panel for later phenotypic and genotypic characterization is outlined in Fig 1A.

The NAB01 primary isolate was first adapted to replication on PBMC in the absence of neutralizing antibody pressure to allow later dissection of sequence alterations due solely to adaptation to CD4^{low} levels [84]. After 39 weeks of adaptation to PBMC culture, the envelope gene of the NAB01 PBMC-adapted (PA) virus, termed NAB01-PA, was cloned, and inserted into

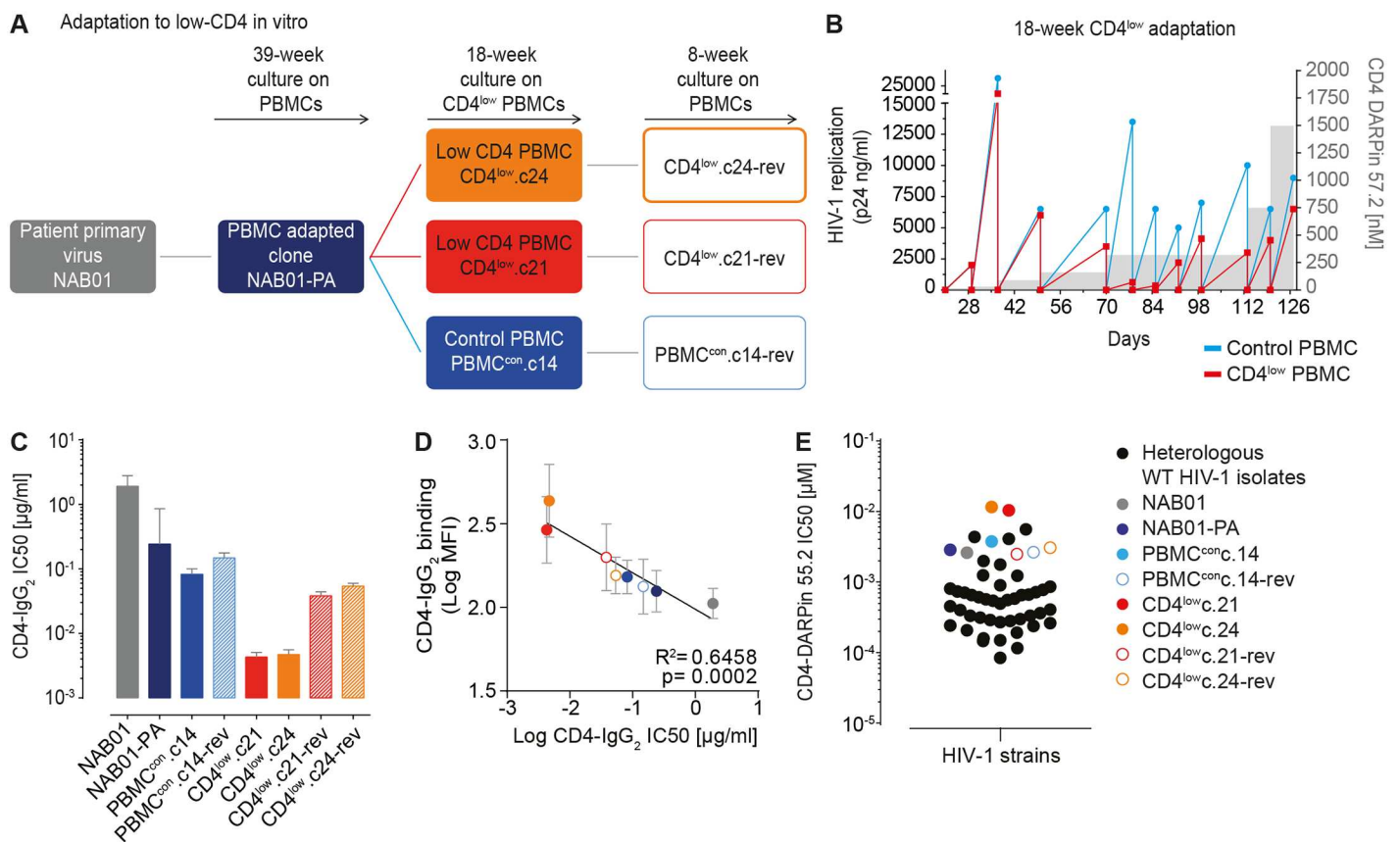


Fig 1. Directed evolution of HIV-1 to utilize CD4^{low} target cells. Adaptation of HIV-1 to CD4^{low} targets *in vitro* (A, B). (A) Overview of stepwise adaptation to CD4^{low} PBMC targets and PBMC reversion cultures with normal CD4 levels and the derived envelope clones. (B) Summary of the 18 week adaptation to low CD4 expressing target cells. Stepwise decrease in available cell surface CD4 on PBMC was achieved by dose escalation of the CD4 inhibitor DARPin 57.2 (right axis, grey shaded areas). HIV-1 replication as measured by p24 antigen production in culture supernatant on CD4 inhibitor treated cells (CD4^{low} culture, red) and control culture (untreated PBMC, blue) are shown. (C) Adaptation to CD4^{low} targets increases sensitivity to CD4-IgG₂ (PRO542). Mean neutralization sensitivity (IC50) of envelope-pseudotyped viruses on TZM-bl cells derived from two to seven independent assays (error bars = SD) are shown. (D) High sensitivity to CD4-IgG₂ is paired with high binding capacity of CD4-IgG₂ to Env trimer. Simple linear regression analysis of CD4-IgG₂ inhibitory capacity (IC50 values shown in panel C) and binding of CD4-IgG₂ to the envelope of the indicated viruses expressed on 293-T cells. Mean fluorescence intensity = MFI. Data are means of two independent experiments; error bars = SD. (E) Adaptation to CD4^{low} target cells results in high resistance to CD4 inhibitor compared to wild type HIV-1 isolates. Comparison of IC50 of CD4-blocking DARPin 55.2 against 41 wild-type HIV-1 strains from different clades (black dots, see S3 Table for details on virus panel and individual IC50 values) and the CD4^{low} adaptation virus panel (colored dots, see legend) probed by Env pseudovirus infection on TZM-bl cells. Data are means of one to three independent experiments.

doi:10.1371/journal.ppat.1006255.g001

the replication competent TN6 HIV vector backbone [85] to produce the Env-chimeric virus NAB01-PA-TN6 as a control in a previous study [84]. The NAB01-PA Env clone carried culture adaptation mutations found previously in independent NAB01 long-term culture viruses (S2 Fig and [84]). Our *in vitro* target cell setup with low CD4 availability was designed to mimic a CD4^{low} target cell environment in an immunological sanctuary site that is not, or only sub-optimally, reached by neutralizing antibodies, as occurs in the CNS. Employing the NAB01-PA envelope pre-adapted to growth in PBMC *in vitro* in absence of an autologous neutralization response allowed us to study the virus envelope evolution in response to alteration of the CD4 availability in the target cell environment in the following steps.

To mimic a CD4^{low} environment, we cultured NAB01-PA-TN6 on PBMC in the presence of the CD4 inhibitor DARPIn 57.2 which competitively interferes with gp120-CD4 binding and thus limits the availability of CD4 on PBMC without interfering otherwise with the cells [75]. Virus was cultured over 18 weeks in the presence of increasing concentrations of DARPIn 57.2 or in absence of the inhibitor. The concentration of DARPIn 57.2 was incrementally increased during the cultivation period from 15 nM at the start, to a final concentration of 1500 nM after 18 weeks of culture (Fig 1B). Functional envelope clones capable of free-virus infection were isolated from both the CD4-DARPIn treated and control culture supernatants (S2 Table). Two unique envelopes, referred to as CD4^{low}.c21 and CD4^{low}.c24, were chosen for further analysis. CD4^{low}.c24 represented the dominant emerged variant representing the bulk sequence of the CD4 DARPIn treated culture, whereas CD4^{low}.c21 differed from this main sequence in several positions (S2 Table). Two functional envelopes were isolated from the corresponding PBMC control culture and, one PBMC^{con}.c14, with high similarity to the bulk sequence and thus representing the main variant, was selected for further characterization (S2 Table).

We next probed if the adaptation to low CD4 levels on target cells results in a stable virus phenotype or if the envelope reverts to wild type once reintroduced into a high CD4 expressing environment. The selected envelope clones of the adaptation and control cultures (CD4^{low}.c21, CD4^{low}.c24, and PBMC^{con}.c14) were re-cloned into the TN6 vector and cultured independently for eight weeks on PBMC in the absence of CD4 inhibitors (termed reversion culture). Functional envelopes representing the main variants were cloned from each reversion culture, and referred to as CD4^{low}.c21-rev, CD4^{low}.c24-rev, and PBMC^{con}.c14-rev (S2 Table) and used to create Env pseudoviruses and Env chimeric TN6 viruses. In sum we compiled a panel of eight envelopes derived from the original patient isolate NAB01 which we refer to as the CD4^{low} adaptation panel, that include the wild type NAB01 Env, the culture adapted control Envs (NAB01-PA, PBMC^{con}.c14, PBMC^{con}.c14-rev), the CD4^{low} adapted Envs (CD4^{low}.c21 and CD4^{low}.c24), and reversion Envs (CD4^{low}.c21-rev and CD4^{low}.c24-rev).

Affinity to CD4 dramatically increases with adaptation to CD4^{low} T cells

To explore if the adaptation to a CD4^{low} environment changed the virus's interaction with CD4, we first compared the sensitivity of our CD4^{low} adaptation panel to the tetrameric fusion protein CD4-IgG₂, also known as Pro-542 [86] (Fig 1C). As high sensitivity to CD4-IgG₂ denotes a high affinity of the HIV-1 envelope for CD4 [78], changes in sensitivity allowed us to directly monitor a functional impact of the adaptation to lower CD4 levels. *In vitro* culture adaptation to PBMC is known to result in an increased sensitivity to CD4 based inhibitors [87–89]. In line with this, we observed a 7.9-fold increase in sensitivity to CD4-IgG₂ for NAB01-PA compared to the patient isolated NAB01. The descendant culture adapted clones PBMC^{con}.c14 and PBMC^{con}.c14-rev only slightly increased their sensitivity further (2.9-fold and 1.6-fold compared to wildtype, respectively), highlighting that NAB01-PA was optimally

adapted to *in vitro* PBMC replication (Fig 1C). In contrast, CD4^{low} pressure resulted in a dramatic increase in sensitivity to CD4 inhibition for both CD4^{low}.c21 and CD4^{low}.c24 with IC50 values 446.3- and 407- fold lower than wildtype (56.5- and 51.5-fold increased sensitivity relative to NAB01-PA), respectively, confirming that these viruses have increased their affinity to CD4 (Fig 1C). However, this high affinity to CD4 was not maintained upon re-exposure to a high CD4 target cell environment on untreated PBMC. Both viruses partially reverted and lost 8.9- and 11.5- fold sensitivity to CD4-IgG₂ compared to the CD4^{low} clones, for reversion culture clones CD4^{low}.c21-rev and CD4^{low}.c24-rev, respectively. This suggested a possible fitness deficit associated with the ability to use low levels of CD4.

To further define the viruses' affinity for CD4 we compared the binding of CD4-IgG₂ to cell surface-expressed envelope trimers by flow cytometry. The geometric mean fluorescence of cell-bound CD4-IgG₂ inversely correlated with CD4-IgG₂ neutralization activity ($R^2 = 0.6458$, $p = 0.0002$; Fig 1D, simple linear regression) confirming that the CD4^{low} adapted strains, which portray high sensitivity to soluble CD4 neutralization, do indeed have an increased affinity for CD4. In line with this heightened affinity for CD4, the CD4^{low} viruses were the least sensitive to CD4-inhibition compared to 41 wild type HIV-1 strains from multiple subtypes (Fig 1E and S3 Table).

CD4 and CCR5 levels influence differential infection capacity of CD4^{low} adapted strains

To elucidate the impact of the altered interaction with the CD4 receptor, we next analyzed how CD4^{low} adapted viruses infect target cells with variable CD4 and CCR5 receptor expression. To this end we utilized the 293-T cell based HIV-1 receptor affinity profiling system (293 Affinofiles) to express 42 unique combinations of CD4 and CCR5 densities (S1 Fig) as previously described [90, 91]. This matrix of receptor expression levels covers relevant *in vivo* CD4 levels and further offers the opportunity to differentiate the influence of CD4 and CCR5 levels independently of each other. In the un-induced stage, Affinofile cells have been shown to express CD4 at 0.7 antibody binding sites (ABS) / μm^2 and at maximal induction 64 CD4 ABS/ μm^2 and therefore to reflect the range of CD4 level distribution observed *in vivo* on monocytes (3.1 CD4 ABS/ μm^2), monocyte derived macrophages (3.4 CD4 ABS/ μm^2) and CD4⁺ T cells (78 CD4 ABS/ μm^2) [21]. We infected induced matrices of Affinofiles and analyzed the 42 independent conditions by 3-D surface plots (S2 Fig).

To assess the efficacy of infection at different receptor densities, we calculated the relative infectivity compared to the maximum activity a given Env reached on Affinofiles for each clone at each Affinofile matrix condition combination (S1 Fig). This analysis highlighted the differential response to decreasing receptor density exhibited by the CD4^{low} adapted Envs in comparison with the rest of the panel (Fig 2). Whereas parental and CD4^{high} target exposed Envs retained only marginal infectivity on targets with low CD4 levels (3% of max for NAB01, NAB01-PA, and PBMC^{con}.c14, 5% for PBMC^{con}.c14-rev), CD4^{low} viruses were markedly higher (18% and 25% for CD4^{low}.c21 and CD4^{low}.c24, respectively) (Fig 2A).

Employing sensitivity vector analysis for Affinofile data [91], we estimated the relative sensitivity of each envelope to changes in CCR5 and CD4 levels. In this analysis, sensitivity vector angles $0^\circ \leq \theta < 45^\circ$ indicate a higher sensitivity to changes in CD4 level, while angles between $45^\circ < \theta \leq 90^\circ$ reflect higher sensitivity to CCR5, and 45° is thereby equal sensitivity to both receptors. In line with an improved capacity to interact with CD4, the CD4^{low} viruses proved to be less steered by changes in CD4 than by CCR5 (57.1° and 60.4° vector for CD4^{low}.c21 and CD4^{low}.c24, respectively; Fig 2B). Comparing the sensitivity vector angles to the parental and control viruses (33.3° - 37.0°) and CD4^{low}-reversion clones (26.8° and 36.9° for CD4^{low}.c21-rev

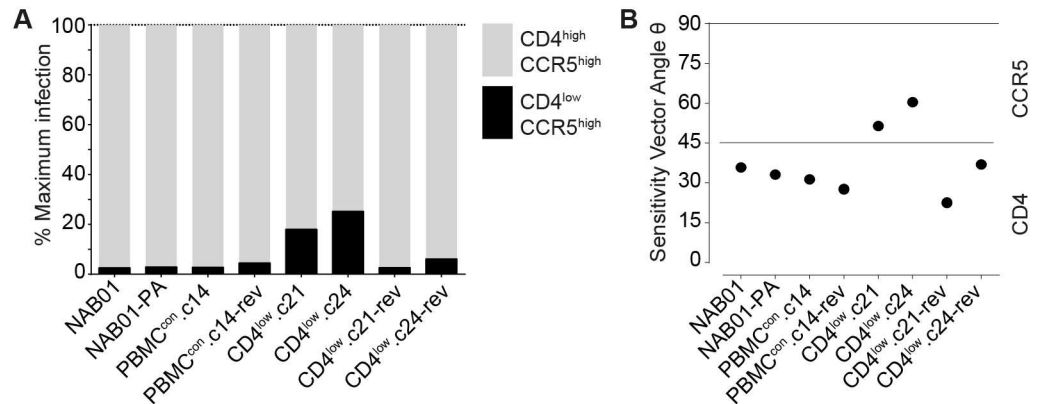


Fig 2. CD4^{low} adapted envelopes infect a wider range of target cells with differential CD4 and/or CCR5 densities. Infection profiles of 293T-Affinofile cells infected with the CD4^{low} panel envelope-pseudotyped viruses. Affinofiles were induced to express a matrix of 42 unique combinations of CD4 and CCR5 and the resulting 3D infection profiles were normalized relative to each envelope's own maximum infection (S1 and S2 Figs). (A) Percent of maximum (high CD4 and high CCR5) level infection retained on cells expressing high CCR5 (2.5 μM Ponasterone A) and the lowest amounts of CD4 (0 μg/ml Doxycycline). Data are from two independent induction and infection assays (S1 and S2 Figs). (B) The VERSA sensitivity vector metrics were calculated by fitting a plane to the 3D surface plots (S2 Fig) as previously described by Johnston et al., 2009, and the resulting vector angle indicates a preferential response to changes in CD4 (angles towards 0°) or CCR5 (angles towards 90°). Vector angles from one of two infection experiments are shown.

doi:10.1371/journal.ppat.1006255.g002

and CD4^{low}.c24-rev, respectively) (Fig 2B), further indicates that the receptor dependency acquired by adaptation to CD4^{low} targets is unfavorable and not stable, as upon replication in a normal CD4 T cell environment, the phenotype is rapidly lost. Control envelopes yielded highly similar values in the vector angle analysis (33.3°-37.0°) suggesting that an optimal dependency for the NAB01 envelope background lies in this range. Of note, the Affinofile sensitivity vector angle was able to elucidate subtle differences in the phenotypes of CD4^{low}.c21-rev and CD4^{low}.c24-rev. The reversion clones displayed differential avenues of compensation for the apparently unfit CD4^{low} adaptation once returned to unrestricted activated PBMC CD4 levels; CD4^{low}.c21-rev showed a markedly lower infectivity compared to CD4^{low}.c24-rev (S2 Fig) and it reverted to even higher dependency on CD4 and lower sensitivity to CCR5 (vector angle 26.8°) than the control viruses (33.3°-37.0°; Fig 2B). In contrast, CD4^{low}.c24-rev recovered infectivity, exhibiting similar levels of infection to the controls on high CD4 cells, and also developed the highest infectivity of the panel on cells with low CD4. These data suggest that CD4^{low} envelopes have adopted a high tolerance for low levels of CD4, with an associated increased utilization of CCR5. CNS macrophage-tropic Env infection of Affinofiles reported similar effects, namely decreased dependence on CD4, altered interaction with CCR5 (compared to paired non-macrophage-tropic envs)[92, 93].

Adaptation to CD4^{low} targets results in marked infectivity loss during free virus infection but not in cell-cell transmission and cell-fusion

We next measured the capacity of the CD4^{low} virus panel to infect target cells with different ranges of CD4 and CCR5 levels using single round replicating Env pseudo-viruses (Fig 3A). We first probed infection on TZM-bl, which were previously estimated to carry 4x10⁵ CD4 and 1.3x10⁴ CCR5 receptors per cell [94], and stimulated PBMC which were estimated to express a pre-activation average of 6x10³ CD4 and 593 CCR5 receptors per cell [29]. In line with the reported receptor densities, we observed higher absolute infectivity on TZM-bl than

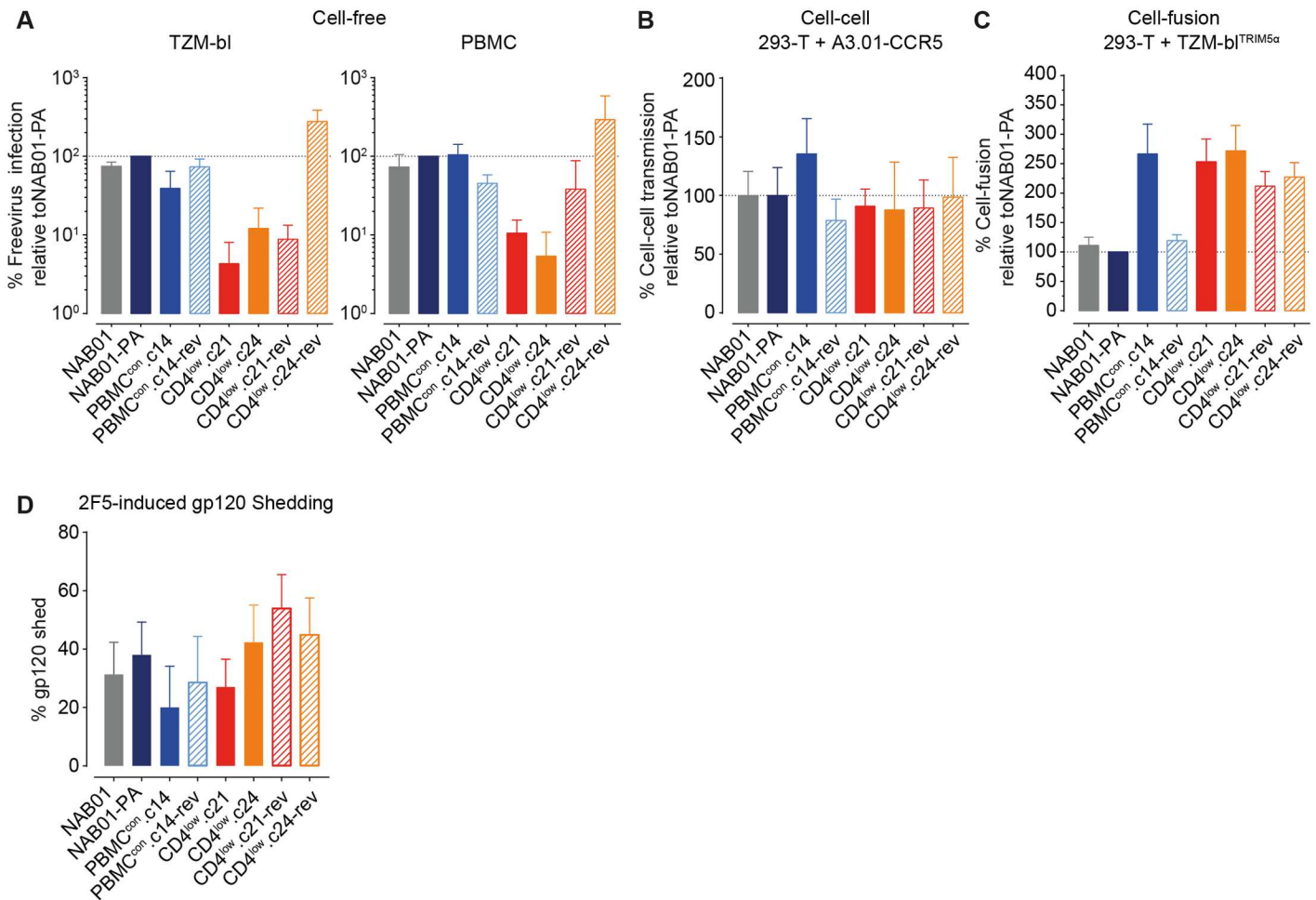


Fig 3. Adaptation to CD4^{low} targets reduces free virus infectivity despite high fusogenicity. (A) Cell-free virus infectivity is reduced upon adaptation to CD4^{low} targets. Infectivity of Env-pseudotyped cell-free virus stocks was assessed by titration on TZM-bl (left) and PBMC (right). Infectivity per unit of p24 capsid was calculated (RLU/ng p24) (S3 Fig) and data expressed as percent infection relative to the parental clone NAB01-PA. Data represent the mean of two to three independent TZM-bl titrations, and the mean of three independent experiments on PBMC using different donor batches of three-way stimulated PBMCs and freshly produced virus stocks. Error bars depict standard deviation (SD). (B) CD4^{low} adapted viruses maintain infectivity during cell-cell transmission. Env and NLinGluc cell-cell transmission reporter expressing 293-T were co-cultured with A3.01-CCR5 cells in the absence of polycation to measure cell to cell transmission capability of the individual envelopes (S3 Fig) as described [95]. Data shown is the mean of two independent assays, error bars are SD. (C) CD4^{low} adapted viruses have high cell-fusion efficacy: Env and NL-Luc-AM reporter expressing 293-T cells were co-cultured with rhesus Trim5α-expressing TZM-bl target cells to measure fusogenicity of panel envelopes. Data shown are the means of three independent assays, error bars are SD. (D) CD4^{low} adapted viruses are not prone to shedding of gp120. Gp120 shedding from Envelope-pseudoviruses in response to treatment with the MPER nAb was assessed as the percentage of gp120 content after 2F5 treatment relative to mock-treated controls normalized to p24 input. Data shown are the means of three independent assays, error bars are SD.

doi:10.1371/journal.ppat.1006255.g003

PBMC (S3 Fig). NAB01, NAB01-PA, and the culture controls PBMC^{con}.c14, and PBMC^{con}.c14-rev, showed infectivity within a 3.6-fold range on both TZM-bl and PBMC (Fig 3). In contrast, adaptation to CD4^{low} targets led to a 2.5–24.8 fold and 3.3–13.3 fold loss in infectivity on TZM-bl and PBMC compared to the parental clone NAB01-PA for CD4^{low}.c21 and CD4^{low}.c24, respectively. Notably, infectivity was restored in only one of the reversion culture clones: CD4^{low}.c24-rev (Fig 3A).

We next explored whether the CD4^{low} adaptation may have led to improved spread in culture via cell-cell transmission to compensate for the attenuated free virus infectivity observed

for CD4^{low}.c21 and CD4^{low}.c24 (Fig 3A). Therefore, we probed the ability of the virus panel to infect via cell-cell transmission (Fig 3B) and to undergo cell-cell fusion (Fig 3C). Cell-cell transmission capacity was similar across the entire virus panel (Fig 3B). The control Env PBMC^{con}.c14 proved to be the most efficient envelope in cell-cell transmission. Most importantly however, we detected no pronounced deficiency for the CD4^{low} adapted strains CD4^{low}.c21 and CD4^{low}.c24, which reached an average of 91% and 88% of the infectivity of NAB01-PA, respectively. This suggested that cell-cell transmission may aid the virus to overcome fitness deficiencies when altering receptor usage. Cell-fusion, however, portrayed an entirely different picture (Fig 3C). The CD4^{low} adapted clones CD4^{low}.c21 and CD4^{low}.c24 together with the control culture envelope PBMC^{con}.c14 were the most effective in initiating fusion, reaching 267%, 253%, and 272% of NAB01-PA, respectively (Fig 3C). Thus, the free virions of the CD4^{low} adapted strains fail to efficiently infect despite intact, if not improved fusogenicity of the Envs.

Decreased free virus infectivity of the CD4^{low} adapted Envs could potentially indicate a low stability of the Env trimers, i.e. trimers that are prone to shed gp120. While Env expressed on the surface of an infected cell is continuously replenished by newly expressed Env, a low stability would affect cell-cell transmission less than free virus infection, where Env on viral particles degrades over time without active replacement. This would fit with the observed pattern of retained cell-cell transmission and low free virus infection. We thus examined the propensity of the Env panel to gp120 shedding in response to the MPER-specific bnAb 2F5, a potent inducer of gp120 shedding [96]. While CD4 induced shedding would also be interesting to define in the context of HIV-1 entry, the large differences in CD4 affinity of the panel nearing a three-log variation in CD4 sensitivity (Fig 1) would not allow for a direct comparison of effects. Measuring 2F5 induced gp120 shedding we observed a modest shedding activity against the CD4^{low} Env clones (27% and 42% for CD4^{low}.c21 and CD4^{low}.c24, respectively) which was in the range of shedding observed for the parental (NAB01) and control (CD4^{low}.c14) envelopes (31% and 20%, respectively). Hence, a high propensity to gp120 shedding cannot be underlying cause of the decreases free-virus infectivity of CD4^{low} compared to parental and control Env clones.

Adaptation to CD4^{low} targets results in infectivity gain on macrophages

High affinity to CD4 has been associated previously with the capacity to infect cells expressing low levels of CD4, in particular macrophages [18, 66, 78, 79, 97, 98]. To test macrophage infectivity we produced two types of differentially conditioned monocyte derived macrophages known to vary in CD4 and CCR5 expression [29], M-MDM have previously been shown to express an average of 125 CD4 and 55 CCR5 receptors per cell while G-MDM have lower levels of both receptors with an estimated 50 CD4 and 15 CCR5 per cell [29]. We verified the relative CD4 expression on our cell preparations and indeed observed 3.1 fold lower CD4 levels on G-MDM (S4 Fig).

As HIV-1 infection of MDM can show high donor variability we verified that the trend observed in Fig 4 was maintained in eight donor cell batches (S4 Fig). Of note, absolute infectivity of ultra-centrifuged Env pseudovirus on M-MDM normalized to p24 content of stocks was close to what we observed for PBMC (S3 and S4 Figs). Overall, G-MDM infection was markedly lower than M-MDM infection (27.4 fold lower NAB01-PA infection on G-MDM than M-MDM; Fig 4A) in line with the lower expression of entry receptors on G-MDM cells.

Interestingly, free-virus infection of M-MDM with the CD4^{low} adapted viruses yielded infection levels closer to parental virus and controls on M-MDM (Fig 4A and 4B) than on PBMC or TZM-bl (Fig 3A) with M-MDM infectivity of CD4^{low}.c21 and CD4^{low}.c24 being

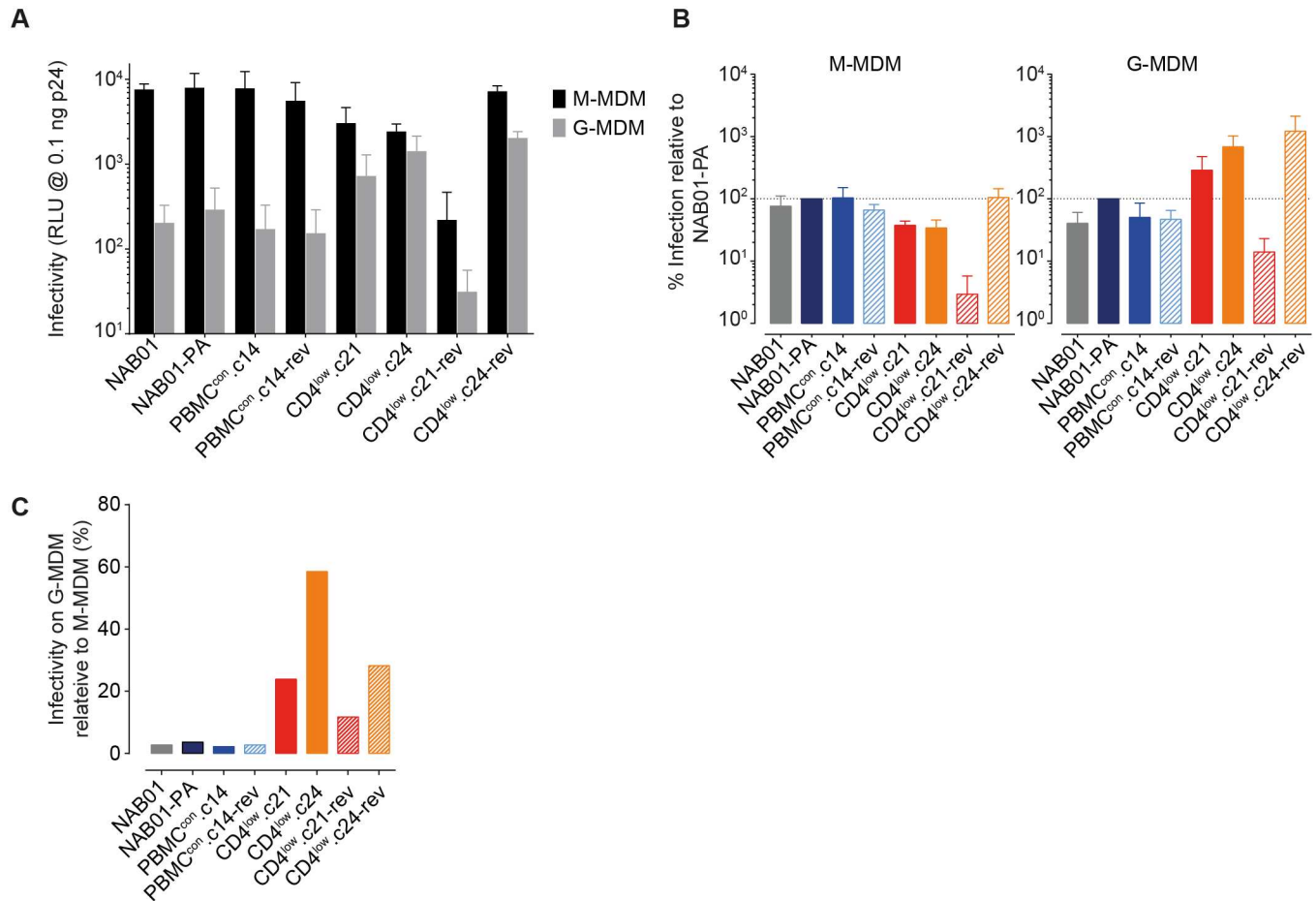


Fig 4. Adaptation to CD4^{low} allows efficient infection of macrophages. (A) Two types of macrophages, M-MDM and G-MDM expressing differential CD4 levels (S4A Fig) were infected with 0.1ng p24 of ultra-centrifuged Env-pseudotyped luciferase reporter virus stocks infection measured on day seven post-infection by quantifying luciferase reporter activity (relative light units (RLU)). Data are means from two individual donors, input of ultracentrifugation purified virus was standardized by p24 content, error bars = SD. (B) Infection of M-MDM and G-MDM by CD4^{low} adapted viruses relative NAB01-PA (data derived from A). (C) Comparison of M-MDM and G-MDM infectivity. Shown is the relative infectivity of G-MDM compared to M-MDM infection (data derived from A).

doi:10.1371/journal.ppat.1006255.g004

only 2.6 and 3.0 fold lower compared to NAB01-PA on, respectively (Fig 4B). The pattern of G-MDM infection was strikingly different. While absolute G-MDM infection was generally lower for all probed viruses (Fig 4A), the CD4^{low} clones infected G-MDM with higher efficiency than the parental and culture control viruses (2.5 fold and 4.9 fold higher compared to NAB01-PA, respectively; Fig 4B). CD4^{low}.c21 and CD4^{low}.c24 reached 23.9% and 58.5%, respectively, of M-MDM infection levels on G-MDM (Fig 4C). In contrast, the parental clone NAB01 showed only 2.7% infectivity on G-MDM compared to M-MDM, similar to NAB01-PA and PBMC^{con}.c14 (3.6% and 2.2%, respectively). Infection of both M-MDM and G-MDM again emphasized the contrasting phenotypes of the two reversion clones. CD4^{low}.c21-rev was the least and CD4^{low}.c24-rev one of the most effective of the entire panel in infection of both MDM subtypes. In sum, the differential infectivity of macrophage subtypes across virus strains supported the observations made using the Affinofile system. Differential macrophage infections further highlighted that adaptation to usage of low CD4 levels can optimize infection of specific cell subsets and thus needs to be considered as an important parameter in shaping target cell tropism throughout disease progression.

Adaptation to low CD4 levels gives rise to envelope mutations associated with macrophage tropism

We next explored the sequence alterations that occurred during adaptation to CD4^{low} pressure (Fig 5 and S4 Table). Locating globally relevant sites of macrophage tropism determination has proven difficult [21]. Numerous mutations have been associated with macrophage tropism

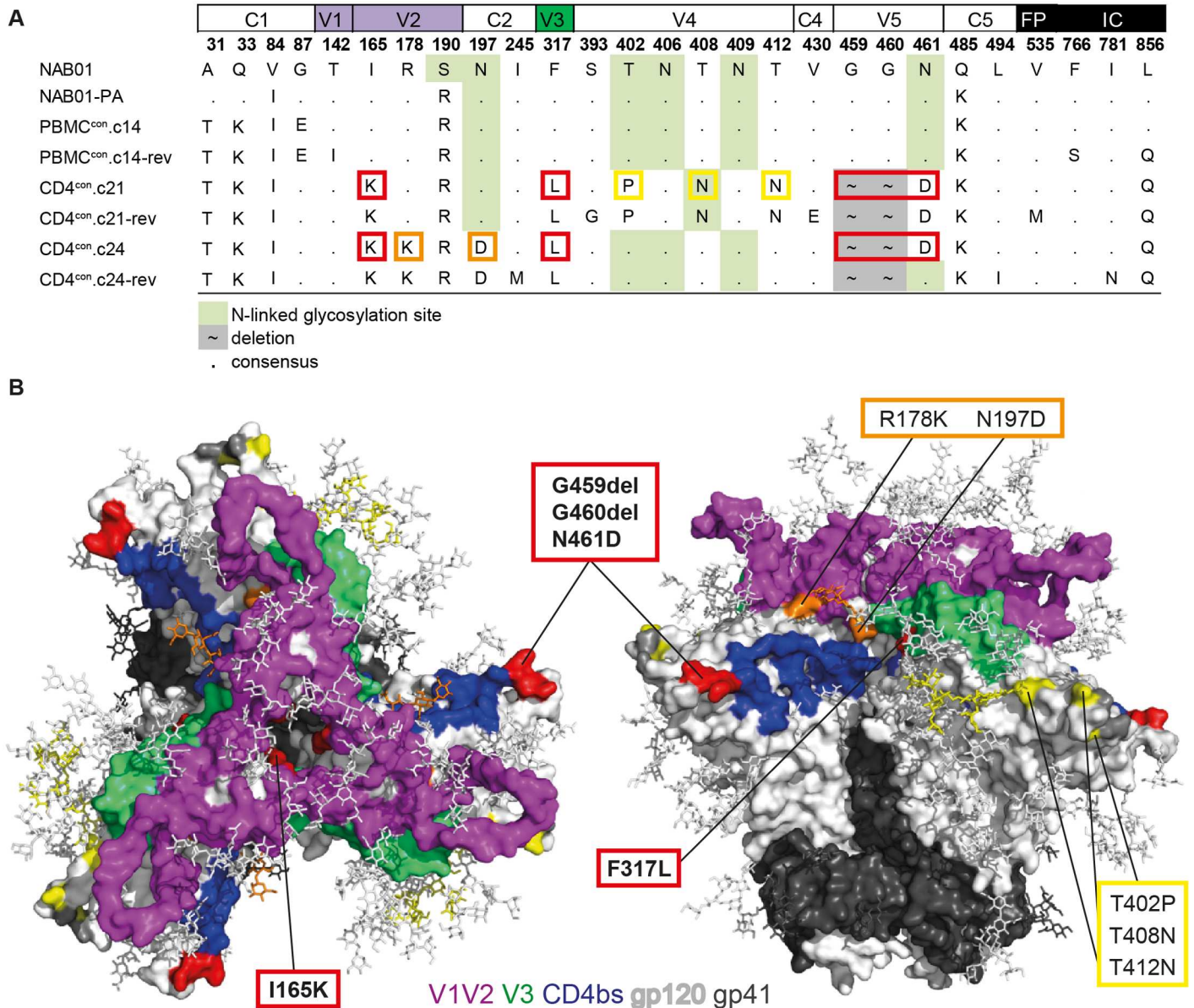


Fig 5. Gp120 sequence mutation pattern following adaptation to CD4^{low} targets. (A) Summary of amino acid mutations acquired as a result of adaptation to long term *in vitro* culture and adaptation to CD4^{low}. Green shading indicates mutations affecting N-linked glycosylation sites. Red boxes denote mutations that occur in both CD4^{low} adapted clones, yellow and orange boxes indicate mutations that occurred only in CD4^{low}.c21 and CD4^{low}.c24, respectively. (B) Structural representations of mutated residues in NAB01 associated with adaptation to low levels of CD4 mapped onto crystal structure 5fyj of X1193.c2 SOSIP [100]. Dark gray residue shading indicates limits of non-resolved region of gp120 V4 loop. Missing from the model are the residue at 402, within the non-resolved region of V4, and the glycans at residues 408 and 461 which are not present on this subtype G Env variant. Structure rendered using PyMol version 1.4.1 [101].

doi:10.1371/journal.ppat.1006255.g005

but were largely found to be strain-specific. Of note, the parental virus NAB01 and all variants derived through culturing lack E153G, T283N, or N386D signatures of enhanced macrophage tropism (reviewed in [14]). CD4^{low} adaptation resulted in five mutations in gp120 common to both CD4^{low}.c21 and CD4^{low}.c24 clones (Fig 5A and S4 Table). The five mutations observed in CD4^{low} Envs include I165K in the V2-loop, F317L in the V3 loop, and in the V5 region a dual deletion at G459 and G460 in combination with N461D that eliminates a potential N-linked glycan at position 461 in the CD4 contact site in V5 [99]. The location of the mutated residues is highlighted on the crystal structure model of subtype G Env trimer X1193.c2 [100] as this structure provides a high resolution of the V4 region (Fig 5B). Although this Env is missing glycans that we found to be under selection pressure in our adapted viruses, overall mapping of the mutated residues onto the X1193.c2 structure provided interesting insights on their approximate spatial distribution.

V2 loop. The mutation I165K is located within the V2 loop in the trimer association area at the apex of the trimer (Fig 5B) and is present in only 0.04% of 4907 envelope sequences analyzed from the Los Alamos Database (S5 Fig). The sequences in this database are dominated by virus derived from plasma and PBMC, and thus are less likely to capture frequencies amongst macrophage or CNS replicating viruses. However, the I165K mutation is found in only 1 of the 98 patients with subtype B Env sequences with CNS ontology included in the HIVbrainseqDB [102], further suggesting that this mutation is rare. In addition to I165K, the V1V2 net charge increased upon adaptation to PBMC from -0.2 to +0.8 and further to +1.8 upon CD4^{low} adaptation. This level of V1V2 charge was sustained for both reversion clones (S4 Table).

V3 loop. No overall net changes in charge of the V3 were observed (S4 Table). The V3-loop mutation F317L that emerged in the CD4^{low} clones is also rare (0.14% of the Los Alamos HIV sequences, 0.06% of subtype B; S5 Fig). F317L has previously been associated with the CD4^{low} adaptation of CNS-derived envelopes [79], and is also prevalent in 14 of 98 patients with CNS derived Subtype B viruses from the HIVbrainseqDB [102]. Residue 317 is located within the highly conserved hydrophobic tip of the V3 loop and has previously been associated with heterodimer stability [103].

CD4bs. The CD4^{low} adapted envelopes shared three mutations proximal to the CD4bs; two deletions in the V5 (G459del, and G460del) and an N461D mutation which eliminates a highly conserved N-linked glycosylation site (found in 99.86% of 4907 sequences in the Los Alamos Database) (S5 Fig). Of the three mutations that the CD4^{low} envelopes shared, N461D was the only one which reverted upon passaging on PBMC with normal CD4 levels in one of the isolated reversion clones (CD4^{low}.c24-rev).

N-glycosylation sites. Both CD4^{low} clones lost further glycosylation sites present in the parental strain (Fig 5A). Mutations T402P, T408N, and T412N present in CD4^{low}.c21 and CD4^{low}.c21-rev are located in a highly variable domain of the V4. These mutations resulted in loss of glycans at positions 402 and 409, and a transfer of an N-linked glycosylation site from 406 to 408. Removal of glycans at 410–412 has been reported to decrease infectivity and increase the potential of the envelope to generate neutralizing antibodies, presumably by exposing neutralization sensitive epitopes [104]. Likewise, N197D, present in both CD4^{low}.c24 and CD4^{low}.c24-rev, destroys a potential N-linked glycosylation site at the apex of the trimer spike known to modulate sensitivity to CD4bs nAbs [105], cause increased CCR5 binding [106, 107] and, in combination with V/T200 (found in all the NAB01 derived clones), has been associated with macrophage tropism in the CNS [108].

Interestingly, by acquiring a L856Q mutation the CD4^{low} adapted clones lose the gp41 C-terminal di-leucine internalization motif thought to play a role in reducing Env content from infected cell surface membranes [109].

High affinity to CD4 is associated with prolonged transitioning during entry from CD4-bound stage to CCR5 engagement and fusion

Altered conformational transitions of the trimer upon receptor engagement have been suggested as an attribute of macrophage-tropic envelopes able to use low levels of CD4 [98]. Considering their increased ability to accomplish membrane fusion (Fig 3C) and to utilize low levels of CD4 to infect (Figs 2A, 2C and 4), we hypothesized that CD4^{low} adaptation may have an influence on the kinetics of attachment and entry.

To assess the relative timing of transitions between the three key steps in the entry process—CD4 engagement, coreceptor binding and fusion—we employed a time-course inhibitor addition experiment with inhibitors targeting CD4 (CD4-DARPin 55.2), CCR5 (maraviroc) and HIV-1 fusion (T-20) (Fig 6A). In this assay setup, synchronized infection is achieved through spinoculation at 4°C (a temperature which prevents receptor engagement) and a shift to 37°C post-spinoculation to initiate entry. Saturating concentrations of inhibitors were added to replicate infection wells at progressive time points from the initiation of infection (0 min) up to 120 min post infection (Fig 6A). For each inhibitor, we considered the relative infectivity compared to the 120 min post infection value and fitted infection curves to estimate the time required by each virus to reach 50% of entry level reached by the 120 min treatment point (Fig 6B).

When comparing the kinetic of the parental NAB01 virus with the two CD4^{low} adapted clones, we observed a striking difference of the times needed to transition from the CD4 bound to the CCR5 bound state as well as from CCR5-to-Fusion (Fig 6C). Whereas the time required to reach 50% fusion differed only 1.4-fold across all eight panel viruses (36.3–50.3 minutes post infection), the time required to complete 50% CD4 binding and 50% CCR5 engagement differed markedly. Most strikingly, we found that the CD4^{low} adapted envelopes, though they engaged CD4 rapidly, required a significant increase in time for the transition between CD4 binding and CCR5 engagement (Mann-Whitney test, $p = 0.00003$ and 0.00024 for comparison between NAB01 and CD4^{low}.c21, NAB01 and CD4^{low}.c24, respectively). While time windows for CD4 and CCR5 binding tightly overlapped for NAB01 and the derived PBMC adapted strains, suggesting a very rapid transition between CD4 and CCR5 engagement for these strains, the CD4^{low}.c21 and CD4^{low}.c24 strains had a time window of 33.2 and 19.6 min between CD4 and CCR5 engagement, respectively. This gap proved largely due to a very rapid initial engagement of CD4 (Fig 6D) and not a postponing of CCR5 binding. In line with their high affinity for CD4, the CD4^{low} adapted envelopes already established a firm CD4 binding during the 30 minute spinoculation at 4°C, reaching a mean of > 40% of the maximal infection (CD4^{low}.c21 at 47.4% and CD4^{low}.c24 at 42.4%; Fig 6C). This was in striking contrast to the rest of the NAB01 virus panel that only reached infection levels between 2.7% and 8.5% before initiation of the entry process by shifting cultures to 37°C. Interestingly, rapid CD4 binding appeared to be an unfavorable trait that the virus only maintained under selection pressure likely as it requires a more open conformation of the trimer. Both reversion clones increased the time to CD4 engagement, and consequently shortened the CD4 to CCR5 transition window.

We then asked whether the phenotype we observed in the CD4^{low} envelope clones could potentially be found *in vivo*, particularly in the CNS where the immune pressure by neutralizing antibodies is less active. To address this question we probed the entry kinetics of a panel of three well established macrophage-tropic envelopes from the CNS (B33 and B59), and plasma (C98-15) together with patient-matched non-macrophage-tropic Envs from lymph nodes (LN40, LN8), and plasma (C98-27) (S5 Table) [64, 76–79]. The rapid engagement of CD4 exhibited by the CD4^{low} Envs was reproduced by the macrophage-tropic

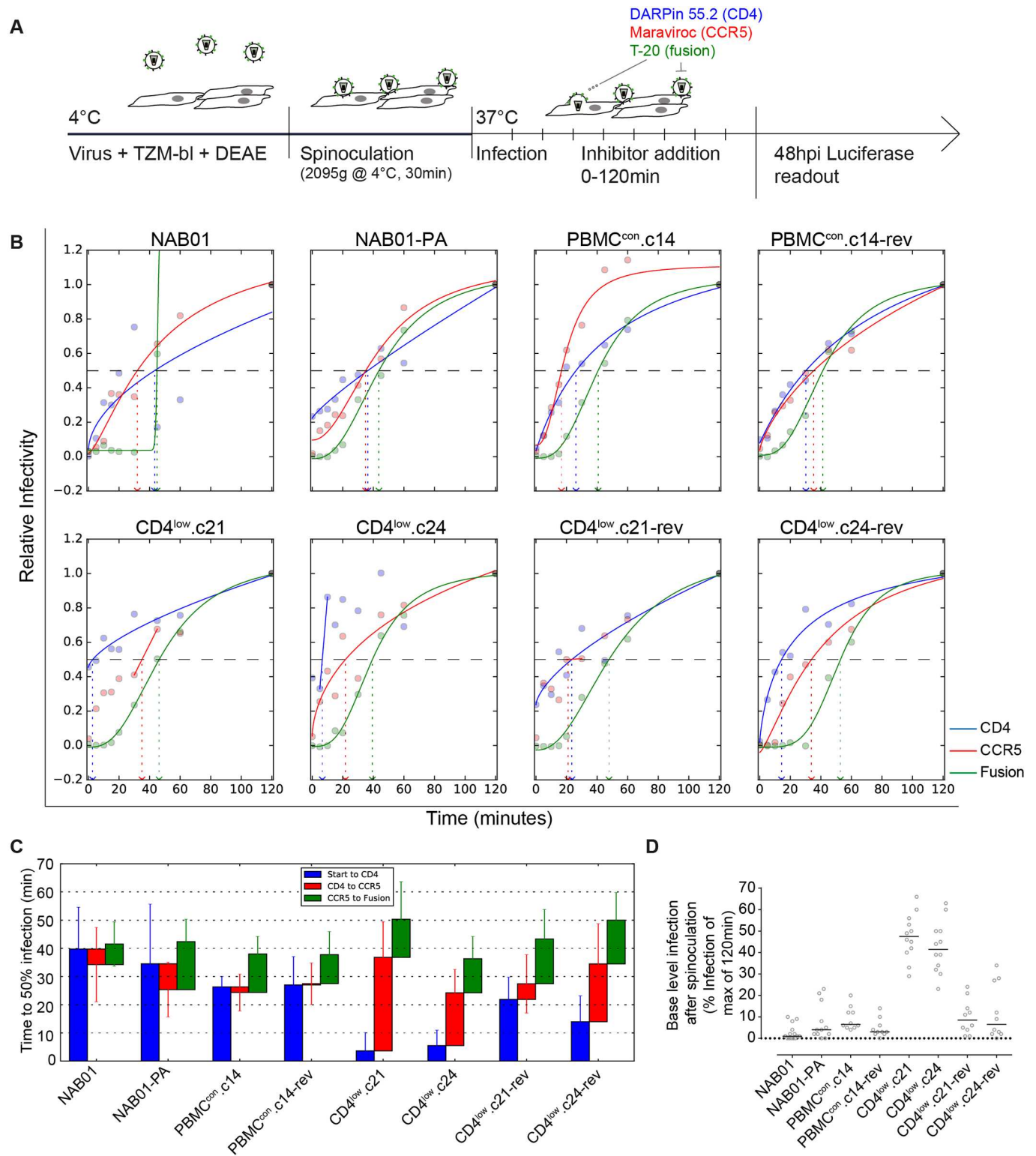


Fig 6. CD4^{low} adapted viruses need extended time to transition between steps in the entry process. (A) Schematic of entry kinetic assay to measure timing of CD4 binding, CCR5 binding, and fusion. Virus is added to TZM-bi in the presence of the polycation DEAE, spinoculated onto cells at 2095g for 30 min at 4°C to limit conformational changes upon CD4 binding. Infection is synchronized by the addition of warmed media and inhibitors targeting CD4 (DARPin 55.2), CCR5 (Maraviroc), and fusion (T-20) added in saturating concentrations at 0, 5, 10, 15, 20, 30, 45, 60, and 120 min post start of infection. (B) For each envelope, one representative time course of infection is shown. Infectivity data are normalized to

infection at 120min post infection and all treatment conditions are shown as relative infectivity compared to this 100% level. **(C)** Definition of transition times required to reach 50% of transition to CD4 bound, CCR5 bound stage and fusion. For each inhibitor and each of at least eight replicate measurements derived from four to six independent experiments, $T_{1/2}$ values of infection times were estimated. The mean of these estimates is a proxy for the time required to reach 50% CD4 resistance, 50% CCR5 resistance, and 50% fusion resistance. Error bars denote SD. **(D)** Percentage of viruses already resistant to CD4 blocking following the 30 minute spinoculation at 4°C. Data points are derived from four to six independent experiments done in replicates. Horizontal bars depict means.

doi:10.1371/journal.ppat.1006255.g006

envelopes (Fig 7A and 7C). The time to CD4 binding for all three patient pairs (B33/LN40, B59/LN8, C98-15/ C98-27) shows a trend of faster CD4 engagement by the macrophage-tropic envelopes when compared to their non-macrophage-tropic paired Env (Fig 7B), though this difference achieves statistical significance only between B33 and LN40 (Fig 7D). Of all patient derived envelopes, the brain-derived B33 also displays the longest CD4 to CCR5 transition (Fig 7B and 7D). The phenotype we observed for CD4^{low} Envs may therefore occur *in vivo*, and in particular in the CNS, where antibody pressure is commonly reduced compared to other compartments. All transitions of the entry process were significantly different between the CD4^{low} clones and NAB01, except time from start to fusion (Fig 7D, Mann-Whitney test). The trends highlighted by the more extreme phenotype of the CD4^{low} envelopes were displayed most similarly by B33, and by B59 and C98-15 to a lesser degree (Fig 7D). To test the sensitivity of our analysis method, we estimated $T_{1/2}$ values in additional ways. First, we averaged the data points from all replicates, prior to fitting only one curve, and since two replicates were always conducted within the same experiment, we also pooled these two data points before fitting the curves and averaging individual $T_{1/2}$ values. Whenever taking the average, we also considered using the median instead of the mean. These different data treatment and analysis methods mostly decreased the power to detect significant differences (S6 Fig), however they had only a minor impact on estimated parameters (S7 Table) and subsequently the trends observed between macrophage-tropic/CD4^{low} compared to non-macrophage-tropic/NAB01 were reproducible.

We further profiled the patient paired macrophage-tropic and non-tropic Env functionality in free-virus infectivity, cell-cell transmission, and cell-fusion to determine the depth of phenotypic similarity shared between CNS-macrophage tropic and CD4^{low} Envs. Interestingly, the infectivity of the CNS-derived macrophage-tropic B33 and B59, but not the plasma-derived C98-15 macrophage-tropic Env was increased relative to their respective non-macrophage tropic control Envs (Fig 8A). The lymph-node derived LN40 and LN8 reached only 12% and 18% of B33 and B59's free-virus infectivity, while C98-15 had half the infectivity of the non-macrophage tropic variant C98-27 (205%). A similar trend was observed in cell-cell transmission where LN40 and LN8 reached 3.5% and 16.5% of the cell-cell capacity of B33 and B59, respectively (Fig 8B). The capacity of all three macrophage-tropic Envs to initiate cell-fusion was similar to the controls, ranging from 98% to 150%, relative to non-macrophage tropic (Fig 8C). Of particular note, all three macrophage-tropic Envs showed an increase in gp120 shedding relative to their paired non-macrophage-tropic Envs, regardless of the tissue of origin (Fig 8D). Both B33 (57%) and B59 (61%) lost more than twice as much gp120 as LN40 (20%) and LN8 (25%). The plasma-derived Envs were more similar, showing 77% and 52% gp120 shedding for C98-15 and C98-27, respectively.

Prolonged transitioning to CCR5 engagement coincides with increased vulnerability to V3 loop and CD4i directed antibodies

We next examined the sensitivity of the virus panel to entry inhibitors and neutralizing antibodies (nAbs) targeting diverse regions of the envelope (S1 Table) to elucidate the consequences of adaptation to low levels of CD4 for shielding and the susceptibility to neutralizing

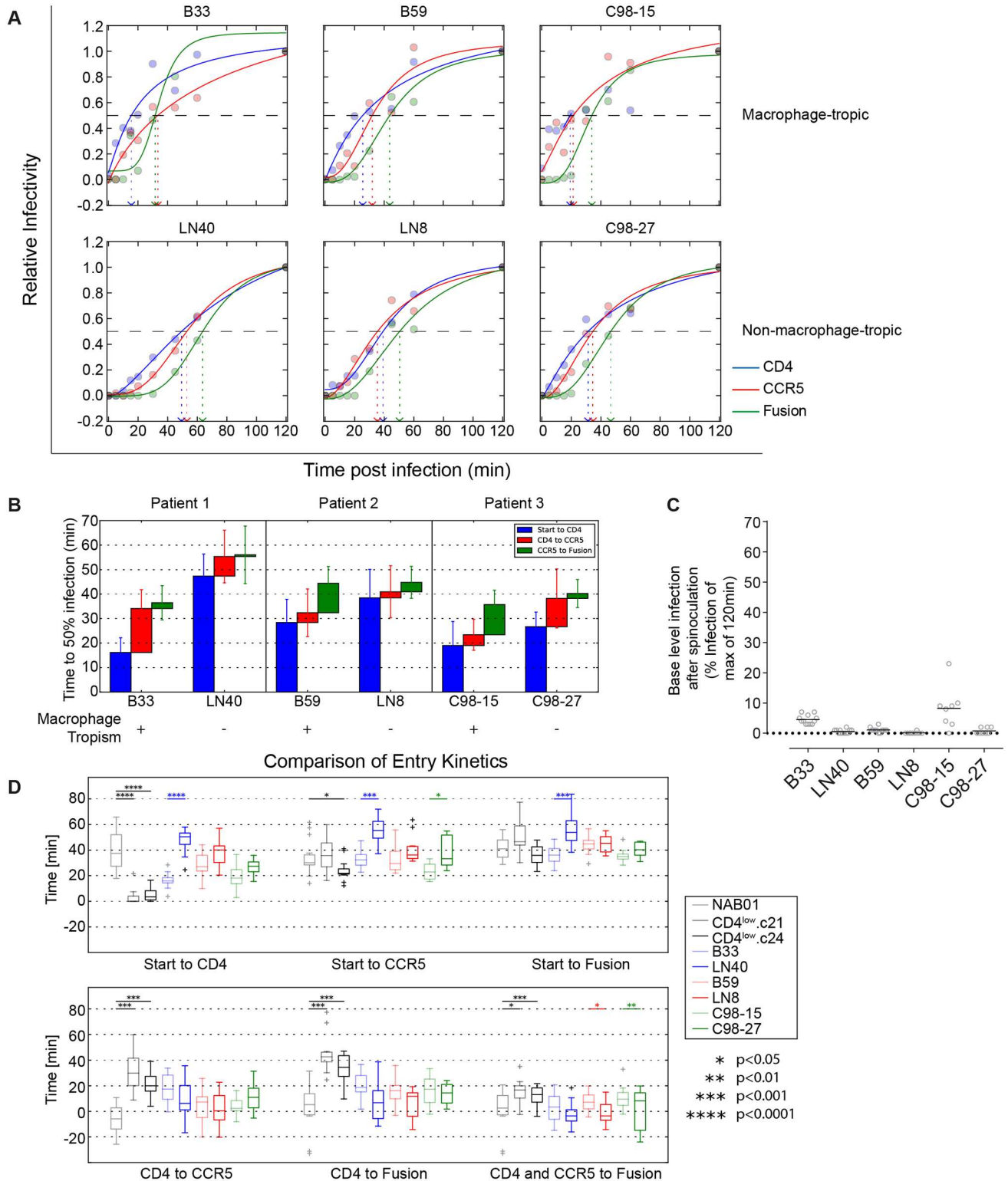


Fig 7. CNS-derived Macrophage-tropic viruses show similar entry pattern with rapid engagement of CD4. (A) to (C) Times to reach 50% resistance to CD4, 50% CCR5, and fusion inhibitors was determined for the shown pairs of patient derived macrophage-tropic and non-macrophage-tropic viruses as described in Fig 6B to 6D. Data for each inhibitor and virus combination were derived from at least eight replicates from four to six independent experiments. (A) For each envelope, one representative time course of infection is shown, normalized to infection at 120min post infection. Data shown is for a replicate representative of the calculated mean of all replicates. (B) Time intervals between four stages of the entry process (synchronized start, CD4 binding, CCR5 attachment, fusion) were compared by Mann-Whitney tests of NAB01 and CD4^{low} viruses and M-tropic and non-M tropic pairs from the analyzed three patients. Only envelopes from the same patient

(same principal color) were compared. **(C)** Data depict the percent of virus already resistant to CD4 blocking following the 30min spinoculation at 4°C. Individual data points are two replicates from each of four to six independent experiments. Horizontal bars depict means. **(D)** Statistical analysis of entry kinetics. Data points from four to six individual experiments were combined before fitting the curves and averaging individual $T_{1/2}$ values. Estimated time intervals between the four stages of the entry process (synchronized start, CD4 binding, CCR5 attachment, fusion) were compared by Mann-Whitney tests. Only envelopes from the same patient (same principal color) were compared. Alternate statistical analysis using paired replicates before curve fitting shown in [S6 Fig](#).

doi:10.1371/journal.ppat.1006255.g007

antibodies. Analysis of the sensitivity of free virus infection to anti-CD4 and CCR5 receptor agents using NAB01-PA as the point of reference highlighted that a modest decrease in sensitivity to CD4 inhibition in the CD4^{low} strains was mirrored by an equally modest increase in sensitivity to the CCR5 inhibitors ([Fig 9A](#) and [S6 Table](#)). This agrees with the higher

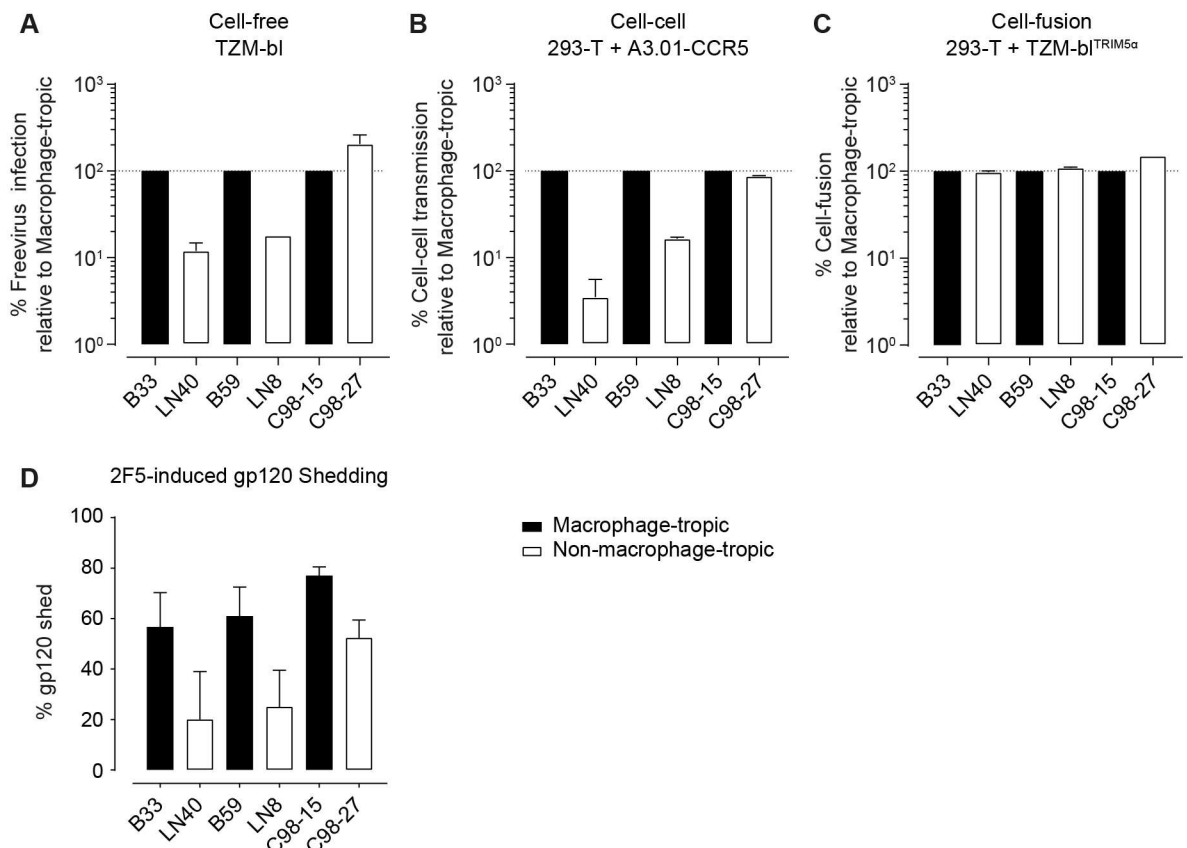


Fig 8. CNS-derived Macrophage-tropic viruses show increased infection capacity and gp120 shedding. **(A)** Cell-free virus infectivity is increased in CNS-derived macrophage tropic Envs. Infectivity of Env-pseudotyped cell-free virus stocks was assessed by titration on TZM-bl. Infectivity per unit of p24 capsid was calculated (RLU/ng p24) ([S7 Fig](#)) and data expressed as percent infection relative to the patient-paired non-macrophage-tropic Env. Data shown is the mean of two independent assays, error bars are SD. **(B)** CNS-derived macrophage-tropic Envs have improved infectivity during cell-cell transmission. Env and NLinGluc cell-cell transmission reporter expressing 293-T were co-cultured with A3.01-CCR5 cells in the absence of polycation to measure cell to cell transmission capability of the individual envelopes ([S7 Fig](#)) as described [[95](#)]. Data shown is the mean of two independent assays, error bars are SD. **(C)** CNS-derived macrophage-tropic Envs maintain similar cell-fusion efficacy to non-macrophage tropic Envs: Env and NL-Luc-AM reporter expressing 293-T cells were co-cultured with rhesus Trim5α-expressing TZM-bl target cells to measure fusogenicity of panel envelopes. Data shown is the mean of two independent assays, error bars are SD. **(D)** CNS-derived macrophage-tropic viruses have increased shedding of gp120. Envelope-pseudoviruses carrying mouse CD4 were treated with 2F5 to induce gp120 shedding and immobilized using magnetic beads. Shed gp120 and non-bound virus was washed away and gp120 and p24 levels measured by ELISA as described [[96](#)]. The difference between gp120 levels of 2F5 treated and to mock-treated controls is depicted as % gp120 shed. Data shown are the means of three independent assays, error bars are SD.

doi:10.1371/journal.ppat.1006255.g008

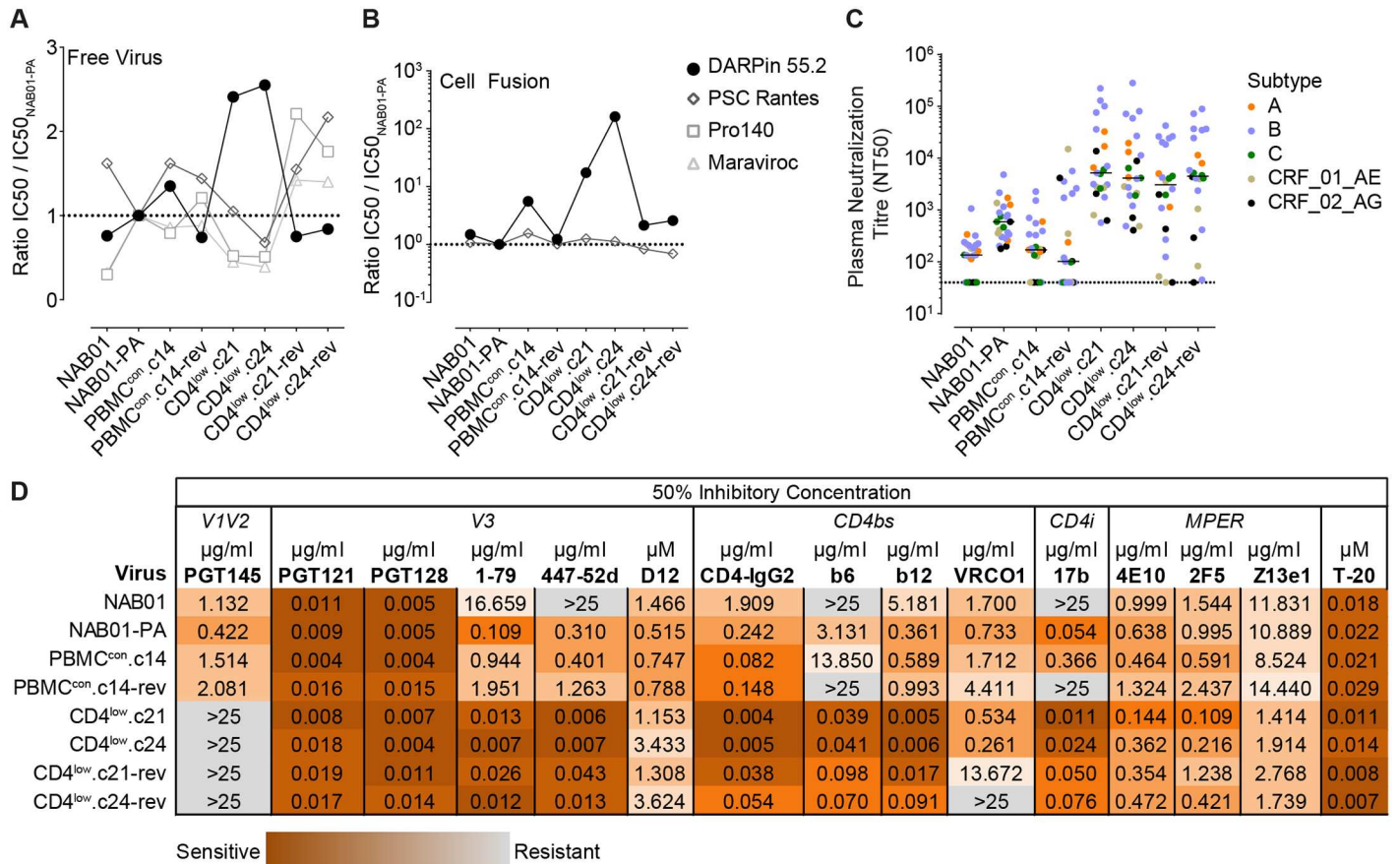


Fig 9. CD4^{low} adapted envelopes show heightened sensitivity to inhibitors targeting the CD4bs, V3 loop, and CD4i epitopes, and patient plasma. (A) and (B) Sensitivity of the CD4^{low} viruses to inhibitors of CD4 (DARPin 55.2) and CCR5 (PSC RANTES, Pro140, Maraviroc). IC50 values are shown relative to the IC50 of NAB01-PA in (A) free virus entry on TZM-bl and (B) 293T-TZMbl^{TRIM5α} cell fusion. Individual IC50 values are listed in S6 Table. (C) Sensitivity of CD4^{low} virus panel to heterologous plasma neutralization. Data are medians derived from neutralization titer on TZM-bl cells of patient plasmas from 24 individuals with different HIV-1 subtype chronic infections (eleven subtype B, four subtype A, and three of each subtype C, 01_AE, and 02_AG). (D) Sensitivity of CD4^{low} virus panel to neutralizing antibodies and Env targeting inhibitors (S1 Table). IC50 values were derived in a standard pseudovirus neutralization assay on TZM-bl cells. Darker shading indicates higher sensitivity. Data shown in A, B, and D are mean values from at least two independent assays for each inhibitor.

doi:10.1371/journal.ppat.1006255.g009

dependency on CCR5 observed in the Affinofile analysis for the CD4^{low} Envs (Fig 2 and S1 and S2 Figs) and was also supported by the observation that the reversion clones lost CCR5 inhibitor sensitivity while regaining sensitivity to CD4 inhibition. Interestingly, the CD4^{low} strains portrayed a much higher resistance to CD4 inhibition during cell-cell fusion while sensitivity to CCR5 inhibition showed no alteration (Fig 9B).

Adaptation of primary isolates to growth *in vitro* in the absence of neutralizing antibody pressure commonly leads to the emergence of virus variants with increased neutralization sensitivity [87]. This was also true for the PBMC long-term cultured NAB01-PA, which displayed higher sensitivity to chronic patient plasma from 24 individuals with chronic HIV-1 infection (eleven subtype B, four subtype A, and three of each subtype C, 01_AE, and 02_AG) (Fig 9C), and nAbs targeting V3, CD4bs, and CD4i (Fig 9D) than the parental NAB01. Sensitivity to V3 glycan and MPER nAbs, and the fusion inhibitor T-20 did not differ between NAB01 and NAB01-PA. In contrast, the V2 glycan nAb PGT145, which depends on a closed trimer conformation for neutralization, showed a 2.7-fold reduced activity against NAB01-PA. CD4^{low} adaptation amplified this phenotype and resulted in a substantial increase in neutralization

sensitivity to nAbs targeting the CD4bs, CD4i, and V3 epitopes, as well as patient plasma (Fig 9C and 9D), ranging from 446-fold (for nAb b6) to 4301-fold (for nAb 447-52d). The V3 targeting DARPIn D12 [110], which recognizes the V3 loop in a structure-dependent manner, slightly decreased in activity against the CD4^{low} and reversion strains compared to NAB01-PA. Similarly, the conformational epitope of PG145 was lost completely in the CD4^{low} envelopes, and was not restored in the reversion clones. Reversion culture viruses also only showed a partial recovery of resistance to V3 and CD4bs nAbs.

Influence of CD4^{low} adaptation on entry stoichiometry

Considering the substantial changes in neutralization sensitivity, entry kinetics, and infectivity across the virus panel, we were next interested to explore if the stoichiometry of entry is altered. It is plausible that the Env conformations which favor CD4 binding that are induced by *in vitro* culture in the absence of neutralization pressure, and adaptation to low levels of CD4 are associated with energetic losses, and in consequence may need more trimers to complete entry [111–113]. To test this, we generated dominant negative Env mutants by introducing R508S/R511S (SEKS) to all panel viruses to knock out the furin-like protease cleavage site between gp120 and gp41, as described [112]. Mixed trimer virus preparations with SEKS variants in varying ratios with wild-type Env were generated and analyzed for infectivity (Fig 10A). Using this data and the average number of trimers per virus particle that was determined in parallel (Fig 10B and S8 Table) allowed us to estimate the minimal number of trimers required for viral entry (T) using a previously established mathematical model [111–113]. While the primary virus NAB01 required only one trimer for entry (T = 1), adaptation to PBMC *in vitro* culture caused an increase of minimal number of trimers required for entry ranging from T = 2 to T = 4. CD4^{low} adaptation maintained T = 4, underlining a continued need for more trimers to be employed in the entry process for these virus variants. The two CD4^{low} reversion clones showed a substantial decrease in the average trimer number per virion, decreasing by 3.7- and 2.8- fold for CD4^{low}.c21-rev and CD4^{low}.c24-rev from their parental clones, respectively. For CD4^{low}.c21-rev this was particularly striking as the average number of trimers per virion (2.1) was lower than the estimated number of trimers required for entry (T = 5). Thus only a small fraction of CD4^{low}.c21-rev virions will carry the required number of trimers necessary to facilitate entry (Fig 10D) and this provides a potential explanation for the particularly low infectivity observed across cell types for (Figs 3A and 4B).

Discussion

During disease progression HIV-1 must overcome the decreasing supply of activated CD4⁺ T cells, which express high levels of CD4 and the CCR5 coreceptor [10, 35, 115, 116]. The transition of the virus to altered receptor usage and the ensuing changes in cell tropism at later disease stages have been extensively studied over the past 30 years, yet many details remain elusive [14, 20, 36, 65, 69–71, 117–120]. The observed transitions during the course of the infection are thought to be needed to allow the virus to infect a broader range of host cells. This may require altered coreceptor usage [15, 77, 121], or modifications to allow infection of cells that express lower CD4 levels. Low CD4 usage in particular is exemplified by R5 viruses exhibiting macrophage tropism [63, 65–67, 74, 77, 78, 98, 122–124]. Development of increased CD4 binding capacity by gp120 has been implicated in high macrophage tropism [125–127], which may have relevant consequences in disease progression (reviewed [128]), however the forces that lead to this phenotype have not been clearly defined. One clue has been provided by the frequent association of highly macrophage-tropic envelopes with CNS infection in late disease [129] suggesting features of this compartment particularly favor or facilitate the

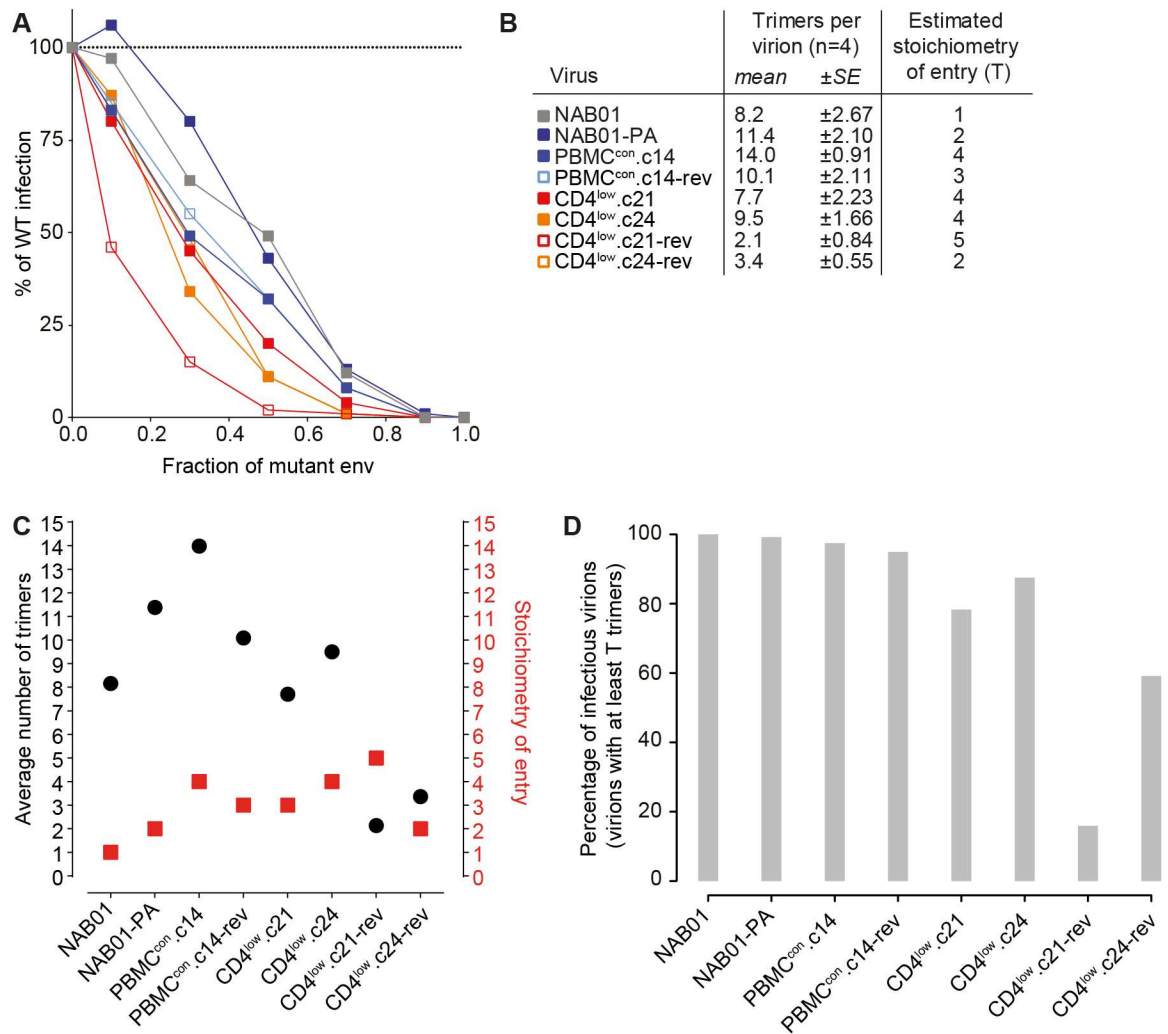


Fig 10. Envelopes adapted to low levels of CD4 require a higher proportion of their available trimers to complete entry. (A) Relative infectivity of mixed trimer infection experiments with CD4^{low} panel viruses using the R508S/R511S dominant-negative Env mutants. Infectivity of pseudotyped virus stocks expressing the indicated ratios of wild type and dominant-negative mutant Envs was measured on TZM-bl reporter cells. Infectivity of virus stocks containing solely the respective WT envelope were set as 100%. Data depict mean from two independent experiments. (B) Experimentally defined mean trimer number per virion measured from four independent assays (S8 Table) were used to derive mathematical estimates of the entry stoichiometry T based on data shown in (A) as described [112]. (C) Graphical presentation of mean trimer number per virion and estimated stoichiometry of entry as shown in (B). (D) The percentage of infectious virions, i.e. virions with at least T trimers, was calculated for each single viral variant based on trimer numbers distributed according to a discretized B-distribution with the measured mean (Fig 10B) as described in [114].

doi:10.1371/journal.ppat.1006255.g010

development of envelopes with high CD4 affinity. Adaptation of the HIV-1 envelope to CD4^{low} conditions warrants study to elucidate potential intermediate evolutionary states, CD4^{low} associated phenotypes, and to improve our understanding of the forces driving development of this niche phenotype at the high end of the continuum of CD4 use.

In the current study we adapted an R5-tropic HIV-1 envelope, isolated from a chronic patient, to CD4^{low} conditions on PBMC *in vitro*. Our setup mimicked the environment that is thought to occur in early infection and the CNS compartment, which is with little or no neutralizing antibody pressure. The ensuing CD4^{low} adapted envelopes displayed a very high affinity binding to CD4. Altered CD4 affinity specifically opens transmission to a new population

of cells via an amplified ability to use low amounts of CD4 on the target cells. While these characteristics suggest an overall benefit to CD4^{low} adaptation, we lay out here that this comes at severe costs for the virus in terms of general infectivity and vulnerability to neutralization.

Adaptation of the NAB01 parental WT envelope to *in vitro* PBMC infection resulted in the S190R and V84I mutations. Herschhorn and colleagues have recently described the impact of mutating the highly conserved leucine at position 190 in the V2 loop [130]. Replacing the L with either an alanine or arginine provided JR-FL (subtype B) and BG505 (subtype A) with improved macrophage infection, increased sensitivity to CD4 binding, and higher neutralization sensitivity by non-neutralizing Abs. Their evidence suggests the mutations enrich the amount of envelopes present in a functional state between the 'closed' wild-type conformation and the CD4-bound 'open' conformation. While NAB01-PA only showed slightly improved macrophage infection, sensitivity to non-neutralizing Abs 1-79, 447-52d, 17b, and b6 were markedly increased, in agreement with an enrichment of the in-between state of envelope conformation.

CD4^{low} adaptation in the NAB01 envelope background occurred by the removal of several structural elements that presumably relaxed restrictions of access for both CD4 and CD4bs specific nAbs. Particularly notable were a deletion of glycosylation sites and part of the V5 loop (affecting residues 459–461) projecting into the space leading to the CD4bs (Fig 5B) [99]. While these changes were linked with an increased ability to bind CD4, the loss of shielding resulted in increased accessibility for CD4bs and CD4i nAbs that are normally well shielded off as exemplified by the increase in efficacy of the CD4bs mAb b6 and the CD4i mAb 17b (Fig 9D). Addition of a positive charge at residue I165K, which comes into close proximity with the neighboring subunits at the trimer association region, has the potential to reduce shielding, by disrupting the interplay of the neighboring V1V2 regions. Mutation of the conserved F317 residue in the V3 is linked with decreased association of gp120 and gp41 [103], further suggesting a decreased conformational stability for the Envs adapted to CD4^{low}.

Our detailed analysis of CD4^{low} envelope entry kinetics further supports a reduction in the energy provided by conformational rearrangements during the multi-step entry process. Following a very rapid CD4 engagement, the time required to transition between steps in the entry process is significantly extended for CD4^{low} adapted envelopes (Figs 6 and 7 and S6 Fig), yet interestingly, the overall length of entry remained comparable. The delay within entry occurs most drastically between binding of CD4 and attachment to CCR5 in the CD4^{low} clones. Given the ability of CD4^{low} Envs to bind to CD4 rapidly and at temperatures normally restrictive to conformational changes, it is surprising that CCR5 attachment does not proceed any quicker, indicating that the CD4^{low} viruses depend on the CCR5 interaction to release the required amount of energy to progression to the next stage of entry. We speculated this may relate to a decreased potential energy carried within the open conformation of the trimers, and could prospectively impact entry stoichiometry. A requirement for a larger number of trimers in order to overcome opposing membrane potentials during entry could help explain the observed delay between CD4 and CCR5 binding. However, the T (stoichiometry of entry) values estimated for CD4^{low} envelopes were comparable to the non-CD4^{low} envelopes adapted to *in vitro* culture, both types requiring four trimers for entry. Notably, the CD4^{low} adapted clones showed a higher T paired with lower overall trimer content on virions. Thus a large fraction of viruses in these populations will not carry the minimal amount of trimers necessary for entry and a high proportion of the available trimers needs to be engaged in the entry process to make infection possible likely explaining the low infectability of these viruses. Whether the CD4^{low} viruses have a CD4 bound conformation that differs from wild type requiring longer to interact with CCR5 or whether this indicates that more CCR5 receptor interactions per trimer have to occur will be further interesting possibilities to explore in future studies.

The *in vitro* adaptation to CD4^{low} targets generated envelope variants with the likely beneficial phenotype of expanded cellular and receptor tropism and drastically increased CD4 binding. However, as mentioned above, the beneficial phenotype comes at the cost of reduced infectivity (Fig 3 and S3 Fig), extended exposure of neutralization sensitive epitopes during entry (Figs 6 and 7), and increased neutralization sensitivity (Fig 9C and 9D). Partial reversion of these phenotypes after readapting to CD4^{high} conditions indicates that an increase in CD4 binding affinity may result in an ultimately less-fit envelope.

The CD4^{low} envelopes proved generally neutralization sensitive in line with the reduced shielding and a prolonged exposure of neutralization sensitive epitopes during entry. It may therefore be critical for this phenotype to develop away from the pressure provided by nAbs *in vivo*. Our examination of CD4^{low} linked phenotypes suggests possible mechanisms that could support development of the neutralization sensitive phenotype. One avenue of adaptation is suggested by our finding that free virus infectivity is dampened for CD4^{low} envelopes but their ability to disseminate via cell-cell transmission is comparable to the primary isolated Env (Fig 3). Maintenance of the cell-cell pathway could potentially serve as a rescue mode of viral transmission supporting previous observations [95, 131, 132]. Cell-cell transmission could thereby allow transmission of less fit virus while adaptation passes through neutralization sensitive intermediates on the way to a more optimally fit phenotype adapted to a CD4^{low} environment. The *in vitro* passaging protocol used in this study is expected to encourage the selection of Envs competent in free-virus infection. Passaging was performed for 16 of the 18 weeks with virus supernatant only. The observed conservation of cell-cell capacity in the face of cell-free selective pressure suggests either a strong impetus to maintain this phenotype, or a lack of effect of the CD4^{low} adaptation and passaging on the cell-cell phenotype. In addition, we expect that the absence of neutralization pressure during *in vitro* passaging allowed the reversion Envs CD4^{low}.c21-rev and CD4^{low}.c24-rev remaining sensitive to neutralization.

In the cell-cell experiment we used one T cell line, A3.01-CCR5 [131], as targets which, as all T cells, has high CD4 levels and is thus comparable to TZM-bl cells in respect to CD4 expression. However, while our data show that a large variation exists in the CD4 use and infectivity of our envelope panel (Figs 1C–1E, 2, 3A and 4), the cell-cell transmission shows little to no difference across the panel. While we cannot rule out that differences in cell-cell transmission may occur when target cells with lower levels of CD4 are involved, in a comparison of CD4^{high} expressing targets only free virus transmission was affected.

In conjunction with competency in cell-cell transmission, the fusion capacity of CD4^{low} envelopes is 2-fold higher than that of NAB01, which may pose a problem to the development of CD4^{low} use *in vivo*. Primarily, cell-fusion does not lead to productive infection and syncytia resulting from cell-fusion may not be long-lived [133]. Therefore, increased fusion in combination with higher CD4 use could result in a dead end path for the virus and thus be a further reason why the virus rarely opts for high CD4 affinity *in vivo*.

The extreme CD4^{low} phenotype was lost during re-adaptation to high CD4 expressing targets even in the absence of nAb pressure. Adaptation to CD4^{low} may therefore encounter resistance from the various fitness related requirements of virus replication *in vivo*. This is supported by the establishment of novel infections by non-macrophage-tropic R5 envelopes [134] due to the fitness costs associated with CD4^{low} use described here, and the bottleneck at transmission selecting high-fitness variants in newly established infections [135]. We have addressed the question of how CD4^{low} envelopes might develop *in vivo* by comparing the entry phenotypes with those of well-defined CD4^{low} using envelopes isolated from patients to find that the CD4^{low} phenotype can be recapitulated amongst viruses replicating in the CNS. It is intriguing that one of the CNS derived envelopes (B33) displayed a phenotype similar to the CD4^{low} adapted clones 21 and 24, while the other (B59) did not. A potential explanation for

this discrepancy could be that B33 and B59 were isolated from CNS at different stages of CNS infection [136] and/or replicated within different cell types [93]. An additional non-competing possibility is that the status of the blood-brain-barrier is affected by the progression of infection [137] differentially in the respective patients, hence allowing more neutralizing antibodies, and/or plasma derived viruses to traverse to the CNS in certain patients. Of the five shared mutations found in both CD4^{low} clones (Fig 5), the only one shared by one of the CNS derived envelopes is 317L which is also found in B33 and has been associated with the ability to use low levels of CD4 [79].

The phenotypic characterization of the CNS-derived macrophage-tropic Envs highlights similarities (e.g. similar entry kinetics) but also differences to our CD4^{low} adapted Envs suggesting that our *in vitro* adapted clones represent an intermediate evolutionary phase with reduced cell-free infectivity. The CNS-derived macrophage-tropic Envs, which displayed superior infectivity in cell-free and cell-cell transmission modes relative to their paired controls (Fig 8), may have passed this stage and acquired compensatory mutations that preserve the entry phenotype but restore infectivity. In particular the elevated infection competency of these CNS-derived Envs despite increased gp120 shedding suggests these Envs have undergone severe selective refinement *in vivo* during their development. It is tempting to speculate that cell-cell transmission *in vivo* may have supported the evolution of these shedding-prone, yet highly infecting competent envelopes. While our *in vitro* selection favored free transmission as only supernatant was passaged, *in vivo* both transmission pathways will be available.

Though the CNS was once considered a site of immunological privilege, it has been established that various branches of the immune system operate within the CNS [138–140] including the production of limited amounts of antibodies from within the cerebrospinal fluid [141]. Envelopes evolving within the CNS may therefore encounter some humoral immune pressure, as B59 may have, though the impact of such an interaction on envelope evolution remains an open question. The lack of an extended entry phenotype in C98-15, isolated originally from plasma, further shows that the phenotype observed is not a universal feature of all highly macrophage-tropic envelopes and may potentially differ depending on whether the clone recently evolved or was circulating (and adapting) for an extended period of time. Nevertheless, the overall trend within each pair of macrophage-tropic and non-macrophage-tropic envelopes mirrors the difference between CD4^{low} adapted and non-adapted Envs from our panel including an increased speed of CD4 binding and extension of transition steps (Fig 7D).

Arrildt and colleagues [125] recently conducted an interesting profiling of phenotypes of primary macrophage-tropic isolates. They found that macrophage-tropic primary isolates were not significantly different from matched control Envs in a variety of functional characteristics including infectivity and entry kinetics, as well as neutralization sensitivity to plasma and V1V2 targeting nAbs. Proposed evolutionary intermediate Envs accordingly showed a moderate sensitivity to CD4. In contrast our CD4^{low} Envs and the CNS-derived macrophage tropic Envs differ from their patient-matched controls. As our Envs, like the CNS-derived macrophage tropic Envs, have not been exposed to humoral immunity during adaptation, it is tempting to speculate that they represent an early adaptive stage that could develop only where humoral immunity is low as in sanctuary sites as the CNS. Infectivity defects, as the CNS derived strains highlight, need not to be associated with this phenotype of CD4^{low} usage and likely are only a transition point in the evolution towards a stable and fit variant.

In summary, adaptation to low levels of CD4 on target cells appears to occur in direct opposition to nAb escape, providing a plausible explanation for the association of highly macrophage-tropic envelopes with the CNS and their appearance before nAb development [80].

Inhibition of the gp120 and CD4 interaction using reagents that bind to the same domain of cellular CD4 that interacts with gp120 to yield effective therapeutics has been investigated extensively [75, 142–145]. Our study, in addition to describing the phenotype resulting from CD4^{low} adaptation, highlights potential routes of escape from CD4 blocking. The envelope adapted to CD4-blocking gains a wider cellular tropism by an increased ability to bind to CD4, raising the possibility that blocking access to CD4 therapeutically could potentially accelerate the generation of envelope variants found normally in late disease stages with increased CD4 binding affinity. The CD4^{low} adapted envelopes generated in our *in vitro* system, as well as one brain-derived envelope (B33) developed high neutralization sensitivity in parallel with CD4 affinity, which suggests for B33 that it may also have developed in the absence of nAb pressure. Intriguingly, a macrophage-tropic isolate derived from plasma (C98-15), which evidently must have been exposed to neutralizing antibodies, retained neutralization resistance despite developing the other features required for macrophage tropism. The same was true for the CNS derived virus B59 opening the possibility that this strain encountered neutralization pressure as well. Both C98-15 and B59 showed a less extreme phenotype in the entry kinetics compared to the CD4^{low} viruses and B33. However, in both cases the same trend in kinetics shift was evident in comparison to non-macrophage-tropic Envs from the same patients (Fig 7). Considering the potential danger of widening the host cell repertoire, administering CD4 derivatives rather than targeting CD4 and the CD4bs directly may be more advisable. That this leads to potent suppression has been shown in the past for CD4-IgG₂ (aka Pro542; [146, 147]), and small-molecule CD4 mimetics [148–151] and with currently unexcelled potency for eCD4-Ig [152]. However, escape pathways for these compounds also need to be meticulously explored to exclude changes in the host cell repertoire and unfavorable alterations in viral fitness. Thus far only few studies have been dedicated to study escape from CD4 mimicking and soluble compounds [153, 154], with more effort defining escape from CD4bs specific Abs elucidating fitness costs associated with escape [155].

In sum our analysis describes a set of phenotypic features directly associated with CD4^{low} adaptation of one subtype B envelope in the absence of nAb pressure that is consistent with phenotypic changes found in two CNS-derived Envs. We have also connected some of these phenotypes to envelopes of primary patient isolates suggesting that the environment where they evolved *in vivo* potentially shares features with the microenvironment we generated *in vitro*. The phenotypic changes that came alongside the adaptation to use low levels of CD4, in particular the alterations in entry kinetics and stoichiometry, trimer content and infectivity may open means to better understand the limitations that evolution of CNS macrophage tropism faces. Mechanistic studies on larger sets of CNS and peripheral macrophages may thus aid to inform vaccine design towards limiting macrophage tropism, ideally preventing the spread of infection into the CNS.

Materials and methods

Ethics statement

Peripheral blood mononuclear cells (PBMC) were purified from buffy coats from anonymous blood donations from healthy individuals obtained by the Zurich Blood Transfusion Service (<http://www.zhbsd.ch/>) under a protocol approved by the local ethics committee.

Patient plasma from twenty-four individuals with chronic HIV-1 subtype A (N = 4), B (N = 11), C (N = 3), CRF_01_AE (N = 3), or CRF_02_AG (N = 3) infections were obtained from biobank samples previously collected during three approved clinical trials the Swiss Spanish treatment interruption trial (SSITT), the Swiss HIV Cohort study (<http://www.shcs.ch>) and the Zurich Primary HIV-infection (ZPHI) study (ClinicalTrials.gov identifier

[NCT00537966](#)) [156–160]. Written informed consent was obtained from all individuals according to the respective studies as stated in the quoted publication according to the guidelines of Canton Zurich and the local ethics committee of all participating clinics.

Reagents

We thank the following individuals for providing inhibitors, antibodies and antibody expression vectors either directly, or via the NIH AIDS Research and Reference Reagent Program (NIH ARP): W. Olsen (Progenics, Tarrytown, New York, USA) for CD4-IgG₂ and PRO140; D. Burton (The Scripps Research Institute, La Jolla, California, USA) for b6, b12, PGT121, PGT128, PGT145, Z13eI; J. Mascola (VRC, Bethesda, Maryland, USA) for VRC01; M. Nussenzweig (The Rockefeller University, New York, USA) for 1–79; J. Robinson (Tulane University, New Orleans, USA) for 17b; D. Katinger (Polymun Scientific, Vienna, Austria) for 2G12, 4E10, and 2F5; and Marc Connors (NIC, Bethesda, Maryland, USA) for 10E8. 447–52d was purchased from Polymun Scientific, Vienna, Austria; T-20 from Roche Pharmaceuticals, Basel, Switzerland; and Maraviroc from Pfizer, UK. Human CD4 specific DARPins 55.2 and 57.2 were expressed as described (Schweizer, Rusert et al. 2008 [75]). A detailed list of all inhibitors and antibodies with their specifications can be found in [S1 Table](#).

Cell lines

293-T cells (American Type Culture Collection (ATCC)) and TZM-bl cells ([161], obtained from the NIH ARP) were cultivated in DMEM with 10% heat inactivated FCS and 1% Penicillin/Streptomycin. Rhesus Monkey Trim5 α expressing TZM-bl cells (TZM-bl^{rhTRIM5 α}) were generated as described [131]. A3.01-CCR5 cells [131] were maintained in RPMI with 10% heat inactivated FCS and 1% Penicillin/Streptomycin. Affinofile cells [90, 91] were thawed every two months and maintained in DMEM media supplemented with 10% dialyzed fetal bovine serum and 50 μ g/ml Blasticidin (Invitrogen, Massachusetts, USA).

Peripheral Blood Mononuclear Cells (PBMC)

Healthy donor PBMC were isolated from buffy coats and stimulated as described [162] and cultivated in RPMI with 10% heat inactivated FCS, 1% Penicillin/Streptomycin and 100 units/ml (U) human recombinant IL-2 (Hoffmann-La Roche, Basel, Switzerland).

NAB01 and NAB01-PA envelopes and generation of Env-chimeric, replication competent TN6 viruses

The cloning of the CCR5-tropic subtype B envelope NAB-01 (previously described as NAB1pre-cl_39x (GenBank database entry [EU023918](#); (<http://www.ncbi.nlm.nih.gov/GenBank/index.html>); [84]), which was derived from the virus isolate of a chronic infected individual, patient NAB01 [82], has been previously described [84, 162]. After 39 weeks of adaptation of the NAB01 isolate to PBMC culture, envelope genes of the adapted virus were cloned from culture supernatant. One clone, termed NAB01 PBMC-adapted (PA), was selected for follow up as representative culture adapted clone as it harbored mutations in V84I and S190R, that were previously observed in PBMC adaptation of NAB01 clones ([84] and EF643665, EF643666, EF643668-EF643670, EF643673-EF643675). The Env NAB01-PA was then cloned into the replication competent TN6 HIV vector backbone [85] to produce the Env-chimeric virus NAB01-PA-TN6 [84] which was used as starting point for the CD4^{low} adaptation. Of note, chimeric envelopes inserted into the TN6 backbone receive the signal peptide and first three amino acids of Env from the original TN6 NL4-3 Env.

Adaptation of NAB01-PA to CD4^{low} expressing target cells

To follow the evolution of NAB01-PA in a low CD4 environment, NAB01-PA-TN6 was passaged on PBMC in the presence of increasing concentrations of a CD4 inhibitor, the high-affinity CD4-binding DARPin 57.2 that efficiently blocks HIV-1 gp120 binding to CD4 [75]. In a parallel control culture, NAB01-PA-TN6 was propagated on the same batches of PBMCs in the absence of the CD4 blocking agent. After 18 weeks of culture and a final maximal concentration of 1.5 μ M DARPin 57.2 (Fig 1B), several functional envelope clones capable of free-virus TZM-bl infection were isolated from both the CD4-DARPin treated and control culture supernatants by RT-PCR (S2 Table). Two unique envelopes, CD4^{low}.c21 and CD4^{low}.c24, representing the main mutation patterns observed, were selected for further follow up (S2 Table). To study whether the phenotype of the derived CD4^{low}.c21 and CD4^{low}.c24 clones is stable or reverts to wild type once back in a CD4 high environment, CD4^{low}.c21, CD4^{low}.c24 and PBMC^{con}.c14 TN6 chimeras were further cultured for eight weeks on untreated PBMCs in the absence of CD4-binding DARPin. After eight weeks, functional envelope genes were isolated from each of the reversion cultures, and representative clones referred to as CD4^{low}.c21-rev, CD4^{low}.c24-rev and PBMC^{con}.c14-rev (rev = reversion culture) chosen for follow up. All envelopes selected for follow up were cloned into pcDNA3.1 expression vector (Invitrogen, Carlsbad, California, USA) as described [84] to allow phenotypic characterization of cell expressed envelopes and Env-pseudoviruses (see below) and further cloned into the TN6 vector to create replication competent chimera.

Patient derived paired macrophage and non-macrophage-tropic envelopes

The previously described patient-derived paired macrophage and non-macrophage-tropic envelopes (B33, LN40/B33, B59, LN8, C98-15, and C98-27 [64, 76–79]) were re-cloned from pSVIII plasmids into pcDNA3.1 expressions plasmids by AT-overhang ligation to allow direct comparison with the CD4^{low} virus panel.

Envelope pseudotyped HIV-1 luciferase reporter virus

Envelope pseudotyped HIV-1 were produced as described [162]. Briefly, 293T cells were transfected with pcDNA3.1 plasmids encoding the respective envelope genes and the Luciferase expressing HIV-1 backbone pNLuc-AM (gift from A.J. Marozsan and J.P. Moore) at a ratio of 1:3 using polyethylenimine (PEI, linear 25 kDa, Polysciences, Eppelheim, Germany). After 8–16h of transfection, medium was replaced with fresh culture medium. Pseudovirus supernatant was collected 48h post transfection and filtered through 20 μ m pore micro filters. Filtrates were then either stored at -80°C or ultra-centrifuged at 49'000g and 4°C for 90 minutes and suspended in PBS before being stored at -80C. Envelope-pseudotyped virus expressing mouse CD4 was produced as previously described [96].

Pseudovirus inhibition assays

Pseudovirus inhibition assays were performed using TZM-bl cells and PBMC as previously described [162, 163]. Briefly, serial dilutions of inhibitors were pre-incubated with target cells or viruses depending on target epitope, for 1hr at 37°C, then virus, cells, and inhibitor were added together and incubated for 48–72 hours. Infection supernatants were then aspirated, cells lysed, luciferase substrate (Promega, Madison Wisconsin, USA) added and the presence of luciferase quantified by measuring relative light units (RLU) using a Dynex MLX 96-well plate reader.

CD4 binding activity of Env variants

To estimate CD4 binding activity of Env variants, we performed a cell-based envelope binding assay. 293-T cells were transfected with pCMV-*rev* and envelope encoding pCDNA3.1 plasmids in a 1:4 ratio with polyethylenimine (PEI, linear 25 kDa, Polysciences, Eppelheim, Germany) and incubated for 36 hours to induce membrane expression of the envelope. CD4 binding activity of cell surface expressed Env was analyzed by flow cytometry using biotin labelled CD4- IgG₂ and detection with streptavidin-PE (BD, New Jersey, USA).

Monitoring dependence on receptor levels by infection of Affinofile cells

CD4 and CCR5 dual-expressing 293-T Affinofile cells were induced and infected in a matrix layout as previously described [90, 91]. Briefly, 1.2×10^5 or 1×10^4 cells were seeded per well of a 24-well culture plate for quantitative flow cytometry of CD4 and CCR5 expression levels, or 96-well clear-bottom culture plate for infections, respectively, and allowed to adhere overnight before being treated with perpendicular serial dilutions of Doxycycline (Sigma Aldrich, Missouri, USA) and Ponasterone A (Invitrogen, Massachusetts, USA) to induce CD4 and CCR5 expression, respectively. Surface expression levels of CD4 and CCR5 were quantified between 18-24h post induction by quantitative flow cytometry using QuantiBRITE beads and PE-labelled antibodies specific for CD4 (clone Q4120; Sigma Aldrich, Missouri, USA) and CCR5 (clone 2D7; BD Biosciences, New Jersey, USA). Affinofile cells were infected 18-24hrs post-induction using 10^5 RLU of virus per well (calculated by titration on TZM-bl cells) in the presence of 10 µg/ml Diethylaminoethyl (DEAE; Amersham plc, UK) and luciferase readout was performed after 48hrs of infection.

Cell-cell transmission

To specifically measure viral infectivity in cell-cell transmission, we employed a recently described A3.01-CCR5 cell based assay [95]. Briefly, this assay utilizes an NL4-3 derived pseudotyped HIV-1 backbone with an intron-regulated Gaussia luciferase LTR-reporter construct called inGluc which is co-transfected with an Env expression plasmid into 293-T donor cells [13, 16, 164], a kind gift from Dr. M Johnson. The reverse orientation of the reporter and the intron allow luciferase expression only after correct splicing, packaging into viral particles and infection of and expression in the A3.01-CCR5 target cells. Free virus infection was restricted by the omission of DEAE in the infection medium as described previously [131].

To measure infectivity in free virus and cell-cell transmission, 2.5×10^5 293-T cells per 6-well were transfected with Env expression plasmid and NLinGluc backbone for cell-cell in a 1:3 ratio, using polyethylenimine (PEI) as transfection reagent. To test cell-cell infectivity, the cells were detached after six hours of incubation and 5×10^3 cells were seeded in 100 µl per 96 well. 1.5×10^4 A3.01-CCR5 target cells in 100 µl RPMI medium were added to the 293-T cells per 96 well. After 60 h of incubation at 37°C, Gaussia luciferase activity in the supernatant was quantified using the Renilla Luciferase Assay System (Promega, Madison Wisconsin, USA) according to the manufacturer's instructions.

Cell fusion assay

We employed a co-culture of HIV-1 pseudovirus transfected 293-T cells and the LTR-firefly luciferase reporter expressing TZM-bl cells to obtain information on the fusion potential of the probed envelope clones. To limit influence of free virus in the readout, we used TZM-bl cells that express rhesus macaque Trim5α, as expression of rhTrim5α in target cells restricts free virus infection [95, 131]. 293-T cells were PEI transfected for six hours with *env*-

pcDNA3.1 and pNL AM GFP backbone. Transfected cells were then detached, washed once at 300g for 3min, suspended in 1200 μ l culture medium and 100 μ l were added to 10 replicate wells of a clear-bottom 96 well plate containing 1.5×10^4 TZM-bl^{rhTrim5 α} in the presence or absence of inhibitors. After 24 hours, luciferase activity was recorded.

Detection of gp120 shedding

Gp120 shedding following treatment with 2F5 was measured as previously described [96]. Envelope-pseudotyped virus carrying mouse CD4 (mCD4) were ultracentrifuged at 49'000g for 90 minutes at 4°C. The virus pellet was resuspended in TBS +2% BSA for 120–200 minutes at room temperature and treated with 100 μ g/ml of mAb 2F5 for 18–20 hours at 37°C. Virions were immobilized with magnetic Dynabeads coated with rat mAb L3T4 specific for mCD4 (Thermo Fisher, Massachusetts, USA) using a magnetic tube rack (DynaMag-2, Thermo Fisher, Massachusetts, USA) and washed twice to remove shed gp120 and non-bound virions. Captured viral particles were lysed with TBS +1% Empigen and gp120 and p24 content measured by ELISA. The gp120 content was normalized to p24 content of each sample and shedding was expressed as a percentage of the mock-treated controls.

HIV-1 infection of primary monocyte-derived-macrophage cultures

Monocytes were purified from freshly isolated healthy donor PBMC using MACS anti-CD14-coated magnetic beads and MACS separation columns (Miltenyi Biotec, Germany). Purity of viable cells ranged between 96–98% as assessed by CD14⁺ staining in flow cytometry (CD14-PE from Life-Technologies; IgG_{2a}-PE Isotype from BD Pharmingen; Live-Dead near infra-red viability stain from Life Technologies; pooled mouse serum used to block fc receptors at 20% (gift of L. Hangartner). 5×10^4 monocytes per well were seeded into 96-well culture plates (Greiner Bio-One GmbH, Germany) for infection experiments, or 2×10^6 cells per well seeded ultra-low attachment surface 6-well plates (Sigma Aldrich, Missouri, USA) for flow cytometry analysis. Monocytes were differentiated for six days in differentiation medium (RPMI1640 supplemented with 1% Pen/strep, 10% fetal-calf serum, 5% pooled human AB serum (Sigma Aldrich, Missouri, USA), 4mM Glutamax (Thermo Fisher, Massachusetts, USA)) and either 100ng/ml M-CSF or 100ng/ml GM-CSF (Immunotools GmbH, Friesoythe, Germany) to produce two different phenotypes of monocyte-derived-macrophages [165–167], known to express differential levels of CD4 and CCR5 [29]. After six days of differentiation @ 37°C in 80% humidity and 5% CO₂, differentiation medium was replaced with culture medium (RPMI 1640, 10% FCS, 1% penicillin and streptomycin) and incubated at 37°C overnight. Pseudovirus infections and flow cytometry of surface receptors were performed on day seven post-isolation. Before infecting MDMs, one well of each MDM type was imaged with an Incucyte ZOOM system using a 10x objective lens and 'scan-on-demand' with the phase contrast channel. Cell morphology was compared to [166] to confirm cultures were independently differentiated as one phenotype or the other by the presence of 'fried egg' morphology for G-MDM, and 'spindle-cells' for M-MDM (S4A Fig). Envelope pseudotyped virus supernatants were titrated onto MDMs and allowed to incubate at 37°C in 80% humidity and 5% CO₂ for seven days. Firefly luciferase production was measured using a Dynex MLX plate reader (high gain setting) and Bright-Glo Luciferase Assay System (Promega, Madison Wisconsin, USA) on day 14 post-isolation (day seven post infection). To analyze surface marker expression, MDM were detached with cell dissociation solution (Sigma Aldrich, Missouri, USA) and stained with CD4-PE (BD, New Jersey, USA), CD195-PE (Biolegend, California, USA, California, USA), CD64-FITC (Biolegend, California, USA), or CD163-BV421 (Biolegend, California, USA) mAbs, or matched isotype controls, to measure expression of HIV receptors CD4 and

CCR5(CD195) and macrophage differential phenotypic markers CD64 and CD163 [168](S4A Fig). Pooled mouse serum (gift of L. Hangartner) was added at 20% to all staining solutions to block unspecific binding of mouse mAbs to MDM Fc receptors.

Envelope sequencing and analysis

Cloned envelope genes were sequenced on an ABI 3130xl genetic analyzer (Applied Biosystems, Rotkreuz, Switzerland) as described [84]. Gp160 protein characteristics were calculated using ProtCalc for charge (<http://protcalc.sourceforge.net/>) and the NIH N-GlycoSite tool (<http://www.hiv.lanl.gov/content/sequence/GLYCOSITE/glycosite.html>) to count potential glycosylation sites. Mutation prevalence in the Los Alamos National Laboratory HIV sequence database was performed using QuickAlign (https://www.hiv.lanl.gov/content/sequence/QUICK_ALIGNv2/QuickAlign.html) web alignment with all 4907 complete sequences available at the time of query. Subtype and Tissue ontogeny- filtered sequences were downloaded from the HIVbrainseqDB [102] and the prevalence of specific mutations queried using a custom algorithm, available on request. Envelope gene sequences of all clones were deposited in the GenBank database entries KX673206-KX673212.

Entry kinetics

Time of inhibitor addition experiments were performed to define entry kinetics with small modifications to previously described protocols [112, 169]. Briefly, 6×10^3 TZM-bl cells in DMEM supplemented with 10 $\mu\text{g}/\text{ml}$ DEAE-Dextran were plated in 384 well clear-bottom plates (Greiner Bio-One GmbH, Germany). Luciferase reporter pseudovirus was spinoculated onto cells for 30min at 2095g and 4°C to settle virus onto cells but prevent receptor engagement. Following spinoculation the supernatant with un-adsorbed virus was removed and 70 μl of 37°C pre-warmed DMEM were added per well to initiate infection (time point zero) and plates were incubated at 37°C. At defined time points post-infection, 10 μl of the respective inhibitor were added to specific wells to stop the viral entry process. Inhibitors (T-20, Maraviroc, and DARPIn 55.2) were added at saturating concentrations (final concentrations of 50 $\mu\text{g}/\text{ml}$, 5 μM and 1 μM , respectively) to ensure inhibition of entry. To obtain a measure for infectivity across different experiments, the wells with the last inhibitor addition at 120 minutes after infection start were used as 100% reference infectivity value and the infectivity of all other inhibitor treated wells were set in relation to it. In addition, a mock-treated well (addition of 10 μl DMEM at time point zero) was evaluated to assess absolute infectivity in absence of inhibitors. Luciferase reporter readout was performed after 48hr incubation at 37°C.

The time to reach 50% of the 120min infection ($T_{1/2}$) was used as a surrogate for timing of receptor (CD4 or CCR5) binding or fusion. For each envelope, each inhibitor and each replicate, a general kinetic equation $(A-D)/(1+(x/C)^B) + D$ was fitted to each replicate time series of data points and a $T_{1/2}$ value was estimated from the fitted equation. If the least-squares approximation used to fit the kinetic equation did not converge, a straight line was instead used to estimate $T_{1/2}$. To deal with irregularities of the data, this line connects the data point left of the first point with >50% relative infectivity and the point right of the last point with <50% relative infectivity. The reported $T_{1/2}$ value for each envelope and each inhibitor is the mean $T_{1/2}$ value across all replicates (see Figs 6 and 7). Mann-Whitney tests were performed to compare the time intervals between the four stages of the entry process (synchronized start, CD4 binding, CCR5 attachment, fusion) among different envelopes. Only envelopes derived from the same patient were compared (see Fig 7 and S6 Fig).

To assess the sensitivity of the method used, we estimated $T_{1/2}$ values in two different ways in addition to the method described above (see S7 Table). First, we took the mean or median

of the data points from all replicate experiments prior to fitting only one curve and estimating $T_{1/2}$. Since each experiment always consisted of two replicates, the second method took the mean or median of these two data points, fitted curves to these data, estimated $T_{1/2}$ values for each pair and averaged them across experiments (see [S7 Table](#)). Whenever taking an average, we also considered using the median instead of the mean (see [S7 Table](#)).

Estimating the stoichiometry of entry

The number of envelope glycoproteins required for target cell entry of the studied envelope variants was calculated as previously described [[112–114](#)]. In short, we generated dominant negative envelope genes in the pcDNA3.1 vector by knocking out the furin cleavage site (R508S/R511S). Ratios of the dominant negative mutant and wild-type envelopes were transfected into 293-T cells along with the NL-Luc-AM HIV-1 backbone to generate pseudotyped viral particles carrying varying ratios of functional and non-functional envelopes. Pseudovirus was then titrated on TZMbl target cells and read out after 48hrs using a Dynex MLX plate reader and Bright-Glo Luciferase Assay System (Promega, Madison Wisconsin, USA).

The number of envelope proteins per viral particle was estimated by quantitative ELISA of gp120 and p24, as previously described [[112](#)], and the mean trimer number of each virus variant determined. These data were then used to determine the number of trimers required for entry using the mathematical framework described in [[112–114](#)].

Supporting information

S1 Table. Inhibitors and antibodies.

(TIF)

S2 Table. Overview Env mutation in clones isolated from CD4^{low} and reversion culturing.

(TIF)

S3 Table. Multi-clade virus panel probed for CD4-DARPin 55.2 sensitivity.

(TIF)

S4 Table. CD4^{low} adaptation panel sequence characteristics.

(TIF)

S5 Table. Patient isolate pairs of macrophage- and non-macrophage-tropic envelopes.

(TIF)

S6 Table. Inhibitory activity of CD4 and CCR5 inhibitors against CD4^{low} adapted viruses during free-virus infection and fusion.

(TIF)

S7 Table. Entry kinetics curve fitting sensitivity analysis.

(TIF)

S8 Table. Estimations of trimer number per virion by quantitative gp120 and p24 ELISA ratios.

(TIF)

S1 Fig. Differential infection of Affinofile cells with varying CD4 and CCR5 levels by CD4^{low} adapted viruses. 293-T Affinofiles were induced to express forty-two unique combinations of (A) CD4 and (B) CCR5 levels. Receptor levels were assessed by quantitative flow cytometry. Data are from one of two independent experiments. (C) and (D) Infection of Affinofile matrices. Following receptor induction Affinofiles were infected with the indicated envelope

pseudotyped viruses. For each pseudovirus, infection across the Affinofile matrix was normalized to the maximum infection this virus reached on Affinofiles in an individual experiment. Data from two independent experiments are shown, error bars = SD. (C) Mean percent maximum infections were plotted by CD4 level. Each panel indicates one level of CD4 induction with CCR5 levels increasing from left to right within each cluster of colored bars. (D) Mean percent maximum infections were plotted by CCR5 level. Each panel indicates one level of CCR5 induction with CD4 levels increasing from left to right within each cluster of colored bars. (TIF)

S2 Fig. Three dimensional Affinofile infection profiles. Affinofiles were induced to express forty-two unique combinations of CD4 and CCR5 and infected with the indicated Env-pseudoviruses. Data of the CD4^{low} envelope panel shown in [S1 Fig](#) and primary virus JR-FL for comparison are depicted. Two independent assays are shown. Axes legends are indicated at top right, dotted line projects into the page. (TIF)

S3 Fig. Comparison of free virus, cell-cell transmission and fusion capacity of CD4^{low} adapted viruses. Data correspond to [Fig 3](#) and depict raw RLU values obtained for the depicted experiments (A) Titration of Env pseudoviruses on TZM-bl and PBMC. Infectivity of CD4^{low} adapted viruses in (B) cell-cell transmission and (C) fusion. (TIF)

S4 Fig. Infectivity of CD4^{low} adapted viruses on macrophages. Differentially conditioned monocyte derived macrophage phenotypes and infection. (A) Phenotypic verification of M-MDM and G-MDM preparation by phase contrast morphology and flow cytometry analysis of CD4, CD64 and CD163. Histograms depict one of 2 independent experiments for CD163 and CD64 staining, and one of 4 independent experiments for CD4 staining, dot-plot shows trends of CD4 and CCR5 staining levels for four independently isolated and treated batches of MDM. (B) Envelope pseudotyped virus stocks were freshly produced by transfecting 293-T cells with pcDNA3.1 envelope expression plasmid together with pNLuc-AM backbone and viral stocks titrated on M-MDM and G-MDM of eight different donors. Data show summary of experiments that were normalized either by input volume, RLU value determined by TZM-bl infectivity (RLU/ μ l), or p24 as determined by ELISA of viral stocks. Infection readout was normalized to NAB01. (C) Absolute infectivity of ultracentrifugation purified Env-pseudovirus stocks on differentially M-MDM and G-MDM with virus input normalized by p24 content. Mean, error bars = SD. (TIF)

S5 Fig. Prevalence of key mutations observed upon adaptation to CD4^{low} targets amongst primary viruses recorded in the Los Alamos sequence database. 4907 available Env sequences were analyzed. (TIF)

S6 Fig. Statistical analysis of entry kinetics following paired curve fitting. Alternative analysis of transition time between steps of the entry process of the data depicted in [Fig 7](#). Data points from the two replicates from the same experiment were combined (i.e. paired) before fitting the curves and averaging individual T_{1/2} values. Estimated time intervals between the four stages of the entry process (synchronized start, CD4 binding, CCR5 attachment, fusion) were compared by Mann-Whitney tests. Only envelopes from the same patient (same principal color) were compared. (TIF)

S7 Fig. Comparison of free virus, cell-cell transmission and fusion capacity of patient-matched macrophage tropic and non-macrophage-tropic viruses. Data correspond to Fig 8 and depicts raw RLU values obtained for the (A) titration of Env pseudoviruses on TZM-bl and infectivity of CD4^{low} adapted viruses in (B) cell-cell transmission and (C) fusion. (TIF)

Acknowledgments

We thank Oliver F. Brandenburg, Lucia Reh, and Valentina Vongrad for fruitful discussions, and Benhur Lee for the Affinofile cells. We thank the NIH AIDS reagent program and their contributors, our patients for their commitment and the Members of the Swiss HIV Cohort Study (Aubert V, Battegay M, Bernasconi E, Böni J, Braun DL, Bucher HC, Calmy A, Cavassini M, Ciuffi A, Dollenmaier G, Egger M, Elzi L, Fehr J, Fellay J, Furrer H (Chairman of the Clinical and Laboratory Committee), Fux CA, Günthard HF (President of the SHCS), Haerry D (deputy of "Positive Council"), Hasse B, Hirsch HH, Hoffmann M, Hösli I, Kahlert C, Kaiser L, Keiser O, Klimkait T, Kouyos RD, Kovari H, Ledergerber B, Martinetti G, Martinez de Tejada B, Marzolini C, Metzner KJ, Müller N, Nicca D, Pantaleo G, Paioni P, Rauch A (Chairman of the Scientific Board), Rudin C (Chairman of the Mother & Child Substudy), Scherrer AU (Head of Data Centre), Schmid P, Speck R, Stöckle M, Tarr P, Trkola A, Vernazza P, Wandeler G, Weber R, Yerly S).

Author Contributions

Conceptualization: DB PR AT.

Formal analysis: DB CM CK OZ PR CO KJM HFG AT.

Funding acquisition: AT HFG.

Investigation: DB PR AT.

Methodology: DB PR AT CK CM OZ.

Project administration: AT.

Resources: HFG MJDD PRC.

Software: OZ.

Supervision: AT.

Validation: DB PR AT KJM HFG.

Visualization: DB CK CM.

Writing – original draft: DB AT.

Writing – review & editing: DB PR CM CK JW TU CO OZ MJDD PRC KJM HFG AT.

References

1. Kwong PD, Doyle ML, Casper DJ, Cicala C, Leavitt SA, Majeed S, et al. HIV-1 evades antibody-mediated neutralization through conformational masking of receptor-binding sites. *Nature*. 2002; 420 (6916):678–82. doi: [10.1038/nature01188](https://doi.org/10.1038/nature01188) PMID: [12478295](https://pubmed.ncbi.nlm.nih.gov/12478295/)
2. Weiss RA, Clapham PR, McClure MO, McKeating JA, McKnight A, Dalglish AG, et al. Human immunodeficiency viruses: neutralization and receptors. *Journal of acquired immune deficiency syndromes*. 1988; 1(6):536–41. Epub 1988/01/01. PMID: [2465401](https://pubmed.ncbi.nlm.nih.gov/2465401/)

3. Lynch RM, Tran L, Louder MK, Schmidt SD, Cohen M, Members CCT, et al. The development of CD4 binding site antibodies during HIV-1 infection. *Journal of virology*. 2012; 86(14):7588–95. Epub 2012/05/11. doi: [10.1128/JVI.00734-12](https://doi.org/10.1128/JVI.00734-12) PMID: [22573869](https://pubmed.ncbi.nlm.nih.gov/22573869/)
4. Georgiev IS, Gordon Joyce M, Zhou T, Kwong PD. Elicitation of HIV-1-neutralizing antibodies against the CD4-binding site. *Current opinion in HIV and AIDS*. 2013; 8(5):382–92. Epub 2013/08/09. doi: [10.1097/COH.0b013e328363a90e](https://doi.org/10.1097/COH.0b013e328363a90e) PMID: [23924998](https://pubmed.ncbi.nlm.nih.gov/23924998/)
5. Grossman Z, Meier-Schellersheim M, Sousa AE, Victorino RM, Paul WE. CD4+ T-cell depletion in HIV infection: are we closer to understanding the cause? *Nature medicine*. 2002; 8(4):319–23. Epub 2002/04/03. doi: [10.1038/nm0402-319](https://doi.org/10.1038/nm0402-319) PMID: [11927927](https://pubmed.ncbi.nlm.nih.gov/11927927/)
6. Cooper A, Garcia M, Petrovas C, Yamamoto T, Koup RA, Nabel GJ. HIV-1 causes CD4 cell death through DNA-dependent protein kinase during viral integration. *Nature*. 2013; 498(7454):376–9. Epub 2013/06/07. doi: [10.1038/nature12274](https://doi.org/10.1038/nature12274) PMID: [23739328](https://pubmed.ncbi.nlm.nih.gov/23739328/)
7. Doitsh G, Galloway NL, Geng X, Yang Z, Monroe KM, Zepeda O, et al. Cell death by pyroptosis drives CD4 T-cell depletion in HIV-1 infection. *Nature*. 2014; 505(7484):509–14. Epub 2013/12/21. doi: [10.1038/nature12940](https://doi.org/10.1038/nature12940) PMID: [24356306](https://pubmed.ncbi.nlm.nih.gov/24356306/)
8. Okoye AA, Picker LJ. CD4(+) T-cell depletion in HIV infection: mechanisms of immunological failure. *Immunological reviews*. 2013; 254(1):54–64. Epub 2013/06/19. doi: [10.1111/imr.12066](https://doi.org/10.1111/imr.12066) PMID: [23772614](https://pubmed.ncbi.nlm.nih.gov/23772614/)
9. Pantaleo G, Graziosi C, Demarest JF, Butini L, Montroni M, Fox CH, et al. HIV infection is active and progressive in lymphoid tissue during the clinically latent stage of disease. *Nature*. 1993; 362(6418):355–8. Epub 1993/03/25. doi: [10.1038/362355a0](https://doi.org/10.1038/362355a0) PMID: [8455722](https://pubmed.ncbi.nlm.nih.gov/8455722/)
10. Brenchley JM, Schacker TW, Ruff LE, Price DA, Taylor JH, Beilman GJ, et al. CD4+ T cell depletion during all stages of HIV disease occurs predominantly in the gastrointestinal tract. *The Journal of experimental medicine*. 2004; 200(6):749–59. Epub 2004/09/15. doi: [10.1084/jem.20040874](https://doi.org/10.1084/jem.20040874) PMID: [15365096](https://pubmed.ncbi.nlm.nih.gov/15365096/)
11. Mehandru S, Poles MA, Tenner-Racz K, Horowitz A, Hurlley A, Hogan C, et al. Primary HIV-1 infection is associated with preferential depletion of CD4+ T lymphocytes from effector sites in the gastrointestinal tract. *The Journal of experimental medicine*. 2004; 200(6):761–70. Epub 2004/09/15. doi: [10.1084/jem.20041196](https://doi.org/10.1084/jem.20041196) PMID: [15365095](https://pubmed.ncbi.nlm.nih.gov/15365095/)
12. Doitsh G, Greene WC. Dissecting How CD4 T Cells Are Lost During HIV Infection. *Cell host & microbe*. 2016; 19(3):280–91. Epub 2016/03/11.
13. Janaka SK, Gregory DA, Johnson MC. Retrovirus glycoprotein functionality requires proper alignment of the ectodomain and the membrane-proximal cytoplasmic tail. *Journal of virology*. 2013; 87(23):12805–13. Epub 2013/09/21. doi: [10.1128/JVI.01847-13](https://doi.org/10.1128/JVI.01847-13) PMID: [24049172](https://pubmed.ncbi.nlm.nih.gov/24049172/)
14. Duncan CJ, Sattentau QJ. Viral determinants of HIV-1 macrophage tropism. *Viruses*. 2011; 3(11):2255–79. doi: [10.3390/v3112255](https://doi.org/10.3390/v3112255) PMID: [22163344](https://pubmed.ncbi.nlm.nih.gov/22163344/)
15. Berger EA, Murphy PM, Farber JM. Chemokine receptors as HIV-1 coreceptors: roles in viral entry, tropism, and disease. *Annual review of immunology*. 1999; 17:657–700. Epub 1999/06/08. doi: [10.1146/annurev.immunol.17.1.657](https://doi.org/10.1146/annurev.immunol.17.1.657) PMID: [10358771](https://pubmed.ncbi.nlm.nih.gov/10358771/)
16. Mazurov D, Ilinskaya A, Heidecker G, Lloyd P, Derse D. Quantitative comparison of HTLV-1 and HIV-1 cell-to-cell infection with new replication dependent vectors. *PLoS pathogens*. 2010; 6(2):e1000788. Epub 2010/03/03. doi: [10.1371/journal.ppat.1000788](https://doi.org/10.1371/journal.ppat.1000788) PMID: [20195464](https://pubmed.ncbi.nlm.nih.gov/20195464/)
17. Gorry PR, Sterjovski J, Churchill M, Witlox K, Gray L, Cunningham A, et al. The role of viral coreceptors and enhanced macrophage tropism in human immunodeficiency virus type 1 disease progression. *Sexual health*. 2004; 1(1):23–34. Epub 2005/12/13. PMID: [16335478](https://pubmed.ncbi.nlm.nih.gov/16335478/)
18. Musich T, Peters PJ, Duenas-Decamp MJ, Gonzalez-Perez MP, Robinson J, Zolla-Pazner S, et al. A conserved determinant in the V1 loop of HIV-1 modulates the V3 loop to prime low CD4 use and macrophage infection. *Journal of virology*. 2011; 85(5):2397–405. Epub 2010/12/17. doi: [10.1128/JVI.02187-10](https://doi.org/10.1128/JVI.02187-10) PMID: [21159865](https://pubmed.ncbi.nlm.nih.gov/21159865/)
19. Gorry PR, Zhang C, Wu S, Kunstman K, Trachtenberg E, Phair J, et al. Persistence of dual-tropic HIV-1 in an individual homozygous for the CCR5Δ32 allele. *The Lancet*. 2002; 359(9320):1832–4.
20. Gorry PR, Taylor J, Holm GH, Mehle A, Morgan T, Cayabyab M, et al. Increased CCR5 affinity and reduced CCR5/CD4 dependence of a neurovirulent primary human immunodeficiency virus type 1 isolate. *Journal of virology*. 2002; 76(12):6277–92. Epub 2002/05/22. doi: [10.1128/JVI.76.12.6277-6292.2002](https://doi.org/10.1128/JVI.76.12.6277-6292.2002) PMID: [12021361](https://pubmed.ncbi.nlm.nih.gov/12021361/)
21. Joseph SB, Arrildt KT, Swanstrom AE, Schnell G, Lee B, Hoxie JA, et al. Quantification of entry phenotypes of macrophage-tropic HIV-1 across a wide range of CD4 densities. *Journal of virology*. 2014; 88(4):1858–69. Epub 2013/12/07. doi: [10.1128/JVI.02477-13](https://doi.org/10.1128/JVI.02477-13) PMID: [24307580](https://pubmed.ncbi.nlm.nih.gov/24307580/)

22. Bleul CC, Wu L, Hoxie JA, Springer TA, Mackay CR. The HIV coreceptors CXCR4 and CCR5 are differentially expressed and regulated on human T lymphocytes. *Proceedings of the National Academy of Sciences of the United States of America*. 1997; 94(5):1925–30. PMID: [9050881](#)
23. Dalgleish AG, Beverley PC, Clapham PR, Crawford DH, Greaves MF, Weiss RA. The CD4 (T4) antigen is an essential component of the receptor for the AIDS retrovirus. *Nature*. 1984; 312(5996):763–7. Epub 1984/12/20. PMID: [6096719](#)
24. Klatzmann D, Champagne E, Chamaret S, Gruest J, Guetard D, Hercend T, et al. T-lymphocyte T4 molecule behaves as the receptor for human retrovirus LAV. *Nature*. 1984; 312(5996):767–8. Epub 1984/12/20. PMID: [6083454](#)
25. McDougal JS, Kennedy MS, Sligh JM, Cort SP, Mawle A, Nicholson JK. Binding of HTLV-III/LAV to T4 + T cells by a complex of the 110K viral protein and the T4 molecule. *Science*. 1986; 231(4736):382–5. Epub 1986/01/24. PMID: [3001934](#)
26. Deng H, Liu R, Ellmeier W, Choe S, Unutmaz D, Burkhart M, et al. Identification of a major co-receptor for primary isolates of HIV-1. *Nature*. 1996; 381(6584):661–6. Epub 1996/06/20. doi: [10.1038/381661a0](#) PMID: [8649511](#)
27. Dragic T, Litwin V, Allaway GP, Martin SR, Huang Y, Nagashima KA, et al. HIV-1 entry into CD4+ cells is mediated by the chemokine receptor CC-CKR-5. *Nature*. 1996; 381(6584):667–73. Epub 1996/06/20. doi: [10.1038/381667a0](#) PMID: [8649512](#)
28. Feng Y, Broder CC, Kennedy PE, Berger EA. HIV-1 entry cofactor: functional cDNA cloning of a seven-transmembrane, G protein-coupled receptor. *Science*. 1996; 272(5263):872–7. Epub 1996/05/10.
29. Lee B, Sharron M, Montaner LJ, Weissman D, Doms RW. Quantification of CD4, CCR5, and CXCR4 levels on lymphocyte subsets, dendritic cells, and differentially conditioned monocyte-derived macrophages. *Proceedings of the National Academy of Sciences of the United States of America*. 1999; 96(9):5215–20. Epub 1999/04/29. PMID: [10220446](#)
30. Richardson MW, Jadhowsky J, Didigu CA, Doms RW, Riley JL. Kruppel-like factor 2 modulates CCR5 expression and susceptibility to HIV-1 infection. *Journal of immunology*. 2012; 189(8):3815–21.
31. Wolfs TF, Zwart G, Bakker M, Goudsmit J. HIV-1 genomic RNA diversification following sexual and parenteral virus transmission. *Virology*. 1992; 189(1):103–10. Epub 1992/07/01. PMID: [1376536](#)
32. Scarlatti G, Tresoldi E, Bjorndal A, Fredriksson R, Colognesi C, Deng HK, et al. In vivo evolution of HIV-1 co-receptor usage and sensitivity to chemokine-mediated suppression. *Nature medicine*. 1997; 3(11):1259–65. Epub 1997/11/14. PMID: [9359702](#)
33. Keele BF, Giorgi EE, Salazar-Gonzalez JF, Decker JM, Pham KT, Salazar MG, et al. Identification and characterization of transmitted and early founder virus envelopes in primary HIV-1 infection. *Proceedings of the National Academy of Sciences of the United States of America*. 2008; 105(21):7552–7. Epub 2008/05/21. doi: [10.1073/pnas.0802203105](#) PMID: [18490657](#)
34. Chikere K, Webb NE, Chou T, Borm K, Sterjovski J, Gorry PR, et al. Distinct HIV-1 entry phenotypes are associated with transmission, subtype specificity, and resistance to broadly neutralizing antibodies. *Retrovirology*. 2014; 11:48. Epub 2014/06/25. doi: [10.1186/1742-4690-11-48](#) PMID: [24957778](#)
35. Blaak H, van't Wout AB, Brouwer M, Hooibrink B, Hovenkamp E, Schuitemaker H. In vivo HIV-1 infection of CD45RA(+)CD4(+) T cells is established primarily by syncytium-inducing variants and correlates with the rate of CD4(+) T cell decline. *Proceedings of the National Academy of Sciences of the United States of America*. 2000; 97(3):1269–74. Epub 2000/02/03. PMID: [10655520](#)
36. Clapham PR, McKnight A. HIV-1 receptors and cell tropism. *British medical bulletin*. 2001; 58:43–59. Epub 2001/11/21. PMID: [11714623](#)
37. Tersmette M, Gruters RA, de Wolf F, de Goede RE, Lange JM, Schellekens PT, et al. Evidence for a role of virulent human immunodeficiency virus (HIV) variants in the pathogenesis of acquired immunodeficiency syndrome: studies on sequential HIV isolates. *Journal of virology*. 1989; 63(5):2118–25. Epub 1989/05/01. PMID: [2564898](#)
38. Koot M, Keet IP, Vos AH, de Goede RE, Roos MT, Coutinho RA, et al. Prognostic value of HIV-1 syncytium-inducing phenotype for rate of CD4+ cell depletion and progression to AIDS. *Annals of internal medicine*. 1993; 118(9):681–8. Epub 1993/05/01. PMID: [8096374](#)
39. Shepherd JC, Jacobson LP, Qiao W, Jamieson BD, Phair JP, Piazza P, et al. Emergence and persistence of CXCR4-tropic HIV-1 in a population of men from the multicenter AIDS cohort study. *The Journal of infectious diseases*. 2008; 198(8):1104–12. Epub 2008/09/12. doi: [10.1086/591623](#) PMID: [18783316](#)

40. Simon B, Grabmeier-Pfistershammer K, Rieger A, Sarcletti M, Schmied B, Puchhammer-Stockl E. HIV coreceptor tropism in antiretroviral treatment-naive patients newly diagnosed at a late stage of HIV infection. *AIDS*. 2010; 24(13):2051–8. Epub 2010/07/06. doi: [10.1097/QAD.0b013e32833c93e6](https://doi.org/10.1097/QAD.0b013e32833c93e6) PMID: [20601851](https://pubmed.ncbi.nlm.nih.gov/20601851/)
41. Wilkin TJ, Goetz MB, Leduc R, Skowron G, Su Z, Chan ES, et al. Reanalysis of coreceptor tropism in HIV-1-infected adults using a phenotypic assay with enhanced sensitivity. *Clinical infectious diseases: an official publication of the Infectious Diseases Society of America*. 2011; 52(7):925–8. Epub 2011/03/24.
42. Zhuang K, Finzi A, Toma J, Frantzell A, Huang W, Sodroski J, et al. Identification of interdependent variables that influence coreceptor switch in R5 SHIV(SF162P3N)-infected macaques. *Retrovirology*. 2012; 9:106. Epub 2012/12/15. doi: [10.1186/1742-4690-9-106](https://doi.org/10.1186/1742-4690-9-106) PMID: [23237529](https://pubmed.ncbi.nlm.nih.gov/23237529/)
43. Zhuang K, Finzi A, Tasca S, Shakirzyanova M, Knight H, Westmoreland S, et al. Adoption of an "open" envelope conformation facilitating CD4 binding and structural remodeling precedes coreceptor switch in R5 SHIV-infected macaques. *PloS one*. 2011; 6(7):e21350. Epub 2011/07/16. doi: [10.1371/journal.pone.0021350](https://doi.org/10.1371/journal.pone.0021350) PMID: [21760891](https://pubmed.ncbi.nlm.nih.gov/21760891/)
44. Tersmette M, Lange JM, de Goede RE, de Wolf F, Eeftink-Schattenkerk JK, Schellekens PT, et al. Association between biological properties of human immunodeficiency virus variants and risk for AIDS and AIDS mortality. *Lancet*. 1989; 1(8645):983–5. Epub 1989/05/06. PMID: [2565516](https://pubmed.ncbi.nlm.nih.gov/2565516/)
45. Schuitemaker H, Koot M, Kootstra NA, Dercksen MW, de Goede RE, van Steenwijk RP, et al. Biological phenotype of human immunodeficiency virus type 1 clones at different stages of infection: progression of disease is associated with a shift from monocytoprotropic to T-cell-tropic virus population. *Journal of virology*. 1992; 66(3):1354–60. Epub 1992/03/01. PMID: [1738194](https://pubmed.ncbi.nlm.nih.gov/1738194/)
46. Cashin K, Paukovics G, Jakobsen MR, Ostergaard L, Churchill MJ, Gorry PR, et al. Differences in coreceptor specificity contribute to alternative tropism of HIV-1 subtype C for CD4 + T-cell subsets, including stem cell memory T-cells. *Retrovirology*. 2014; 11(1):97. Epub 2014/11/13.
47. Connor RI, Sheridan KE, Ceradini D, Choe S, Landau NR. Change in coreceptor use correlates with disease progression in HIV-1-infected individuals. *The Journal of experimental medicine*. 1997; 185(4):621–8. Epub 1997/02/17. PMID: [9034141](https://pubmed.ncbi.nlm.nih.gov/9034141/)
48. Connor RI, Mohri H, Cao Y, Ho DD. Increased viral burden and cytopathicity correlate temporally with CD4+ T-lymphocyte decline and clinical progression in human immunodeficiency virus type 1-infected individuals. *Journal of virology*. 1993; 67(4):1772–7. Epub 1993/04/01. PMID: [8095306](https://pubmed.ncbi.nlm.nih.gov/8095306/)
49. Blaak H, Brouwer M, Ran LJ, de Wolf F, Schuitemaker H. In vitro replication kinetics of human immunodeficiency virus type 1 (HIV-1) variants in relation to virus load in long-term survivors of HIV-1 infection. *The Journal of infectious diseases*. 1998; 177(3):600–10. Epub 1998/03/14. PMID: [9498438](https://pubmed.ncbi.nlm.nih.gov/9498438/)
50. Masciotra S, Owen SM, Rudolph D, Yang C, Wang B, Saksena N, et al. Temporal relationship between V1V2 variation, macrophage replication, and coreceptor adaptation during HIV-1 disease progression. *AIDS*. 2002; 16(14):1887–98. Epub 2002/09/28. PMID: [12351948](https://pubmed.ncbi.nlm.nih.gov/12351948/)
51. Tuttle DL, Anders CB, Aquino-De Jesus MJ, Poole PP, Lamers SL, Briggs DR, et al. Increased replication of non-syncytium-inducing HIV type 1 isolates in monocyte-derived macrophages is linked to advanced disease in infected children. *AIDS research and human retroviruses*. 2002; 18(5):353–62. doi: [10.1089/088922202753519133](https://doi.org/10.1089/088922202753519133) PMID: [11897037](https://pubmed.ncbi.nlm.nih.gov/11897037/)
52. Repits J, Sterjovski J, Badia-Martinez D, Mild M, Gray L, Churchill MJ, et al. Primary HIV-1 R5 isolates from end-stage disease display enhanced viral fitness in parallel with increased gp120 net charge. *Virology*. 2008; 379(1):125–34. doi: [10.1016/j.virol.2008.06.014](https://doi.org/10.1016/j.virol.2008.06.014) PMID: [18672260](https://pubmed.ncbi.nlm.nih.gov/18672260/)
53. Duenas-Decamp MJ, Peters PJ, Repik A, Musich T, Gonzalez-Perez MP, Caron C, et al. Variation in the biological properties of HIV-1 R5 envelopes: implications of envelope structure, transmission and pathogenesis. *Future virology*. 2010; 5(4):435–51. Epub 2010/10/12. doi: [10.2217/fvl.10.34](https://doi.org/10.2217/fvl.10.34) PMID: [20930940](https://pubmed.ncbi.nlm.nih.gov/20930940/)
54. Tsao LC, Guo H, Jeffrey J, Hoxie JA, Su L. CCR5 interaction with HIV-1 Env contributes to Env-induced depletion of CD4 T cells in vitro and in vivo. *Retrovirology*. 2016; 13:22. doi: [10.1186/s12977-016-0255-z](https://doi.org/10.1186/s12977-016-0255-z) PMID: [27026376](https://pubmed.ncbi.nlm.nih.gov/27026376/)
55. Parrish NF, Wilen CB, Banks LB, Iyer SS, Pfaff JM, Salazar-Gonzalez JF, et al. Transmitted/founder and chronic subtype C HIV-1 use CD4 and CCR5 receptors with equal efficiency and are not inhibited by blocking the integrin alpha4beta7. *PLoS pathogens*. 2012; 8(5):e1002686. Epub 2012/06/14. doi: [10.1371/journal.ppat.1002686](https://doi.org/10.1371/journal.ppat.1002686) PMID: [22693444](https://pubmed.ncbi.nlm.nih.gov/22693444/)
56. Moore JP, Kitchen SG, Pugach P, Zack JA. The CCR5 and CXCR4 coreceptors—central to understanding the transmission and pathogenesis of human immunodeficiency virus type 1 infection. *AIDS research and human retroviruses*. 2004; 20(1):111–26. Epub 2004/03/06. doi: [10.1089/088922204322749567](https://doi.org/10.1089/088922204322749567) PMID: [15000703](https://pubmed.ncbi.nlm.nih.gov/15000703/)

57. Meyaard L, Otto SA, Jonker RR, Mijster MJ, Keet RP, Miedema F. Programmed death of T cells in HIV-1 infection. *Science*. 1992; 257(5067):217–9. Epub 1992/07/10. PMID: [1352911](#)
58. Finkel TH, Tudor-Williams G, Banda NK, Cotton MF, Curiel T, Monks C, et al. Apoptosis occurs predominantly in bystander cells and not in productively infected cells of HIV- and SIV-infected lymph nodes. *Nature medicine*. 1995; 1(2):129–34. Epub 1995/02/01. PMID: [7585008](#)
59. Perfettini JL, Castedo M, Roumier T, Andreau K, Nardacci R, Piacentini M, et al. Mechanisms of apoptosis induction by the HIV-1 envelope. *Cell death and differentiation*. 2005; 12 Suppl 1:916–23. Epub 2005/02/19.
60. Garg H, Mohl J, Joshi A. HIV-1 induced bystander apoptosis. *Viruses*. 2012; 4(11):3020–43. Epub 2012/12/04. doi: [10.3390/v4113020](#) PMID: [23202514](#)
61. Gorry PR, Ancuta P. Coreceptors and HIV-1 pathogenesis. *Current HIV/AIDS reports*. 2011; 8(1):45–53. Epub 2010/12/29. doi: [10.1007/s11904-010-0069-x](#) PMID: [21188555](#)
62. Parker ZF, Iyer SS, Wilen CB, Parrish NF, Chikere KC, Lee FH, et al. Transmitted/founder and chronic HIV-1 envelope proteins are distinguished by differential utilization of CCR5. *Journal of virology*. 2013; 87(5):2401–11. Epub 2012/12/28. doi: [10.1128/JVI.02964-12](#) PMID: [23269796](#)
63. Martin J, LaBranche CC, Gonzalez-Scarano F. Differential CD4/CCR5 utilization, gp120 conformation, and neutralization sensitivity between envelopes from a microglia-adapted human immunodeficiency virus type 1 and its parental isolate. *Journal of virology*. 2001; 75(8):3568–80. Epub 2001/03/27. doi: [10.1128/JVI.75.8.3568-3580.2001](#) PMID: [11264346](#)
64. Peters PJ, Bhattacharya J, Hibbitts S, Dittmar MT, Simmons G, Bell J, et al. Biological analysis of human immunodeficiency virus type 1 R5 envelopes amplified from brain and lymph node tissues of AIDS patients with neuropathology reveals two distinct tropism phenotypes and identifies envelopes in the brain that confer an enhanced tropism and fusigenicity for macrophages. *Journal of virology*. 2004; 78(13):6915–26. Epub 2004/06/15. doi: [10.1128/JVI.78.13.6915-6926.2004](#) PMID: [15194768](#)
65. Dunfee R, Thomas ER, Gorry PR, Wang J, Ancuta P, Gabuzda D. Mechanisms of HIV-1 neurotropism. *Current HIV research*. 2006; 4(3):267–78. Epub 2006/07/18. PMID: [16842080](#)
66. Thomas ER, Dunfee RL, Stanton J, Bogdan D, Taylor J, Kunstman K, et al. Macrophage entry mediated by HIV Envs from brain and lymphoid tissues is determined by the capacity to use low CD4 levels and overall efficiency of fusion. *Virology*. 2007; 360(1):105–19. Epub 2006/11/07. doi: [10.1016/j.virol.2006.09.036](#) PMID: [17084877](#)
67. Dunfee RL, Thomas ER, Wang J, Kunstman K, Wolinsky SM, Gabuzda D. Loss of the N-linked glycosylation site at position 386 in the HIV envelope V4 region enhances macrophage tropism and is associated with dementia. *Virology*. 2007; 367(1):222–34. Epub 2007/06/30. doi: [10.1016/j.virol.2007.05.029](#) PMID: [17599380](#)
68. Gorry PR, Dunfee RL, Mefford ME, Kunstman K, Morgan T, Moore JP, et al. Changes in the V3 region of gp120 contribute to unusually broad coreceptor usage of an HIV-1 isolate from a CCR5 Delta32 heterozygote. *Virology*. 2007; 362(1):163–78. Epub 2007/01/24. doi: [10.1016/j.virol.2006.11.025](#) PMID: [17239419](#)
69. Gorry PR, Bristol G, Zack JA, Ritola K, Swanstrom R, Birch CJ, et al. Macrophage tropism of human immunodeficiency virus type 1 isolates from brain and lymphoid tissues predicts neurotropism independent of coreceptor specificity. *Journal of virology*. 2001; 75(21):10073–89. Epub 2001/10/03. doi: [10.1128/JVI.75.21.10073-10089.2001](#) PMID: [11581376](#)
70. Gray L, Sterjovski J, Churchill M, Ellery P, Nasr N, Lewin SR, et al. Uncoupling coreceptor usage of human immunodeficiency virus type 1 (HIV-1) from macrophage tropism reveals biological properties of CCR5-restricted HIV-1 isolates from patients with acquired immunodeficiency syndrome. *Virology*. 2005; 337(2):384–98. Epub 2005/05/27. doi: [10.1016/j.virol.2005.04.034](#) PMID: [15916792](#)
71. Sterjovski J, Roche M, Churchill MJ, Ellett A, Farrugia W, Gray LR, et al. An altered and more efficient mechanism of CCR5 engagement contributes to macrophage tropism of CCR5-using HIV-1 envelopes. *Virology*. 2010; 404(2):269–78. Epub 2010/06/24. doi: [10.1016/j.virol.2010.05.006](#) PMID: [20570309](#)
72. DeJucq N, Simmons G, Clapham PR. Expanded tropism of primary human immunodeficiency virus type 1 R5 strains to CD4(+) T-cell lines determined by the capacity to exploit low concentrations of CCR5. *Journal of virology*. 1999; 73(9):7842–7. Epub 1999/08/10. PMID: [10438877](#)
73. Gray LR, Turville SG, Hitchen TL, Cheng WJ, Ellett AM, Salimi H, et al. HIV-1 entry and trans-infection of astrocytes involves CD81 vesicles. *PloS one*. 2014; 9(2):e90620. Epub 2014/03/04. doi: [10.1371/journal.pone.0090620](#) PMID: [24587404](#)
74. Gorry PR, Francella N, Lewin SR, Collman RG. HIV-1 envelope-receptor interactions required for macrophage infection and implications for current HIV-1 cure strategies. *Journal of leukocyte biology*. 2014; 95(1):71–81. Epub 2013/10/26. doi: [10.1189/jlb.0713368](#) PMID: [24158961](#)

75. Schweizer A, Rusert P, Berlinger L, Ruprecht CR, Mann A, Corthesy S, et al. CD4-specific designed ankyrin repeat proteins are novel potent HIV entry inhibitors with unique characteristics. *PLoS pathogens*. 2008; 4(7):e1000109. Epub 2008/07/26. doi: [10.1371/journal.ppat.1000109](https://doi.org/10.1371/journal.ppat.1000109) PMID: [18654624](https://pubmed.ncbi.nlm.nih.gov/18654624/)
76. Peters PJ, Sullivan WM, Duenas-Decamp MJ, Bhattacharya J, Ankghuambom C, Brown R, et al. Non-macrophage-tropic human immunodeficiency virus type 1 R5 envelopes predominate in blood, lymph nodes, and semen: implications for transmission and pathogenesis. *Journal of virology*. 2006; 80(13):6324–32. Epub 2006/06/16. doi: [10.1128/JVI.02328-05](https://doi.org/10.1128/JVI.02328-05) PMID: [16775320](https://pubmed.ncbi.nlm.nih.gov/16775320/)
77. Peters PJ, Duenas-Decamp MJ, Sullivan WM, Clapham PR. Variation of macrophage tropism among HIV-1 R5 envelopes in brain and other tissues. *Journal of neuroimmune pharmacology: the official journal of the Society on NeuroImmune Pharmacology*. 2007; 2(1):32–41. Epub 2007/11/28.
78. Peters PJ, Duenas-Decamp MJ, Sullivan WM, Brown R, Ankghuambom C, Luzuriaga K, et al. Variation in HIV-1 R5 macrophage-tropism correlates with sensitivity to reagents that block envelope: CD4 interactions but not with sensitivity to other entry inhibitors. *Retrovirology*. 2008; 5:5. Epub 2008/01/22. doi: [10.1186/1742-4690-5-5](https://doi.org/10.1186/1742-4690-5-5) PMID: [18205925](https://pubmed.ncbi.nlm.nih.gov/18205925/)
79. Duenas-Decamp MJ, Peters PJ, Burton D, Clapham PR. Determinants flanking the CD4 binding loop modulate macrophage tropism of human immunodeficiency virus type 1 R5 envelopes. *Journal of virology*. 2009; 83(6):2575–83. Epub 2009/01/09. doi: [10.1128/JVI.02133-08](https://doi.org/10.1128/JVI.02133-08) PMID: [19129457](https://pubmed.ncbi.nlm.nih.gov/19129457/)
80. Richards KH, Aasa-Chapman MM, McKnight A, Clapham PR. Modulation of HIV-1 macrophage-tropism among R5 envelopes occurs before detection of neutralizing antibodies. *Retrovirology*. 2010; 7:48. Epub 2010/05/29. doi: [10.1186/1742-4690-7-48](https://doi.org/10.1186/1742-4690-7-48) PMID: [20507591](https://pubmed.ncbi.nlm.nih.gov/20507591/)
81. Dunfee RL, Thomas ER, Gorry PR, Wang J, Taylor J, Kunstman K, et al. The HIV Env variant N283 enhances macrophage tropism and is associated with brain infection and dementia. *Proceedings of the National Academy of Sciences of the United States of America*. 2006; 103(41):15160–5. Epub 2006/10/04. doi: [10.1073/pnas.0605513103](https://doi.org/10.1073/pnas.0605513103) PMID: [17015824](https://pubmed.ncbi.nlm.nih.gov/17015824/)
82. Trkola A, Kuster H, Rusert P, Joos B, Fischer M, Leemann C, et al. Delay of HIV-1 rebound after cessation of antiretroviral therapy through passive transfer of human neutralizing antibodies. *Nature medicine*. 2005; 11(6):615–22. Epub 2005/05/10. doi: [10.1038/nm1244](https://doi.org/10.1038/nm1244) PMID: [15880120](https://pubmed.ncbi.nlm.nih.gov/15880120/)
83. Rusert P, Kuster H, Joos B, Misselwitz B, Gujer C, Leemann C, et al. Virus isolates during acute and chronic human immunodeficiency virus type 1 infection show distinct patterns of sensitivity to entry inhibitors. *Journal of virology*. 2005; 79(13):8454–69. Epub 2005/06/16. doi: [10.1128/JVI.79.13.8454-8469.2005](https://doi.org/10.1128/JVI.79.13.8454-8469.2005) PMID: [15956589](https://pubmed.ncbi.nlm.nih.gov/15956589/)
84. Manrique A, Rusert P, Joos B, Fischer M, Kuster H, Leemann C, et al. In vivo and in vitro escape from neutralizing antibodies 2G12, 2F5, and 4E10. *Journal of virology*. 2007; 81(16):8793–808. doi: [10.1128/JVI.00598-07](https://doi.org/10.1128/JVI.00598-07) PMID: [17567707](https://pubmed.ncbi.nlm.nih.gov/17567707/)
85. Neumann T, Hagmann I, Lohrengel S, Heil ML, Derdeyn CA, Krausslich HG, et al. T20-insensitive HIV-1 from naive patients exhibits high viral fitness in a novel dual-color competition assay on primary cells. *Virology*. 2005; 333(2):251–62. Epub 2005/02/22. doi: [10.1016/j.virol.2004.12.035](https://doi.org/10.1016/j.virol.2004.12.035) PMID: [15721359](https://pubmed.ncbi.nlm.nih.gov/15721359/)
86. Allaway GP, Davis-Bruno KL, Beaudry GA, Garcia EB, Wong EL, Ryder AM, et al. Expression and characterization of CD4-IgG2, a novel heterotetramer that neutralizes primary HIV type 1 isolates. *AIDS research and human retroviruses*. 1995; 11(5):533–9. Epub 1995/05/01. doi: [10.1089/aid.1995.11.533](https://doi.org/10.1089/aid.1995.11.533) PMID: [7576908](https://pubmed.ncbi.nlm.nih.gov/7576908/)
87. Pugach P, Kuhmann SE, Taylor J, Marozsan AJ, Snyder A, Ketas T, et al. The prolonged culture of human immunodeficiency virus type 1 in primary lymphocytes increases its sensitivity to neutralization by soluble CD4. *Virology*. 2004; 321(1):8–22. Epub 2004/03/23. doi: [10.1016/j.virol.2003.12.012](https://doi.org/10.1016/j.virol.2003.12.012) PMID: [15033560](https://pubmed.ncbi.nlm.nih.gov/15033560/)
88. Beaumont T, Quakkelaar E, van Nuenen A, Pantophlet R, Schuitemaker H. Increased sensitivity to CD4 binding site-directed neutralization following in vitro propagation on primary lymphocytes of a neutralization-resistant human immunodeficiency virus IIIB strain isolated from an accidentally infected laboratory worker. *Journal of virology*. 2004; 78(11):5651–7. doi: [10.1128/JVI.78.11.5651-5657.2004](https://doi.org/10.1128/JVI.78.11.5651-5657.2004) PMID: [15140962](https://pubmed.ncbi.nlm.nih.gov/15140962/)
89. Moore JP, Burkly LC, Connor RI, Cao Y, Tizard R, Ho DD, et al. Adaptation of two primary human immunodeficiency virus type 1 isolates to growth in transformed T cell lines correlates with alterations in the responses of their envelope glycoproteins to soluble CD4. *AIDS research and human retroviruses*. 1993; 9(6):529–39. Epub 1993/06/01. doi: [10.1089/aid.1993.9.529](https://doi.org/10.1089/aid.1993.9.529) PMID: [8347397](https://pubmed.ncbi.nlm.nih.gov/8347397/)
90. Chikere K, Chou T, Gorry PR, Lee B. Affinofile profiling: how efficiency of CD4/CCR5 usage impacts the biological and pathogenic phenotype of HIV. *Virology*. 2013; 435(1):81–91. Epub 2012/12/12. doi: [10.1016/j.virol.2012.09.043](https://doi.org/10.1016/j.virol.2012.09.043) PMID: [23217618](https://pubmed.ncbi.nlm.nih.gov/23217618/)
91. Johnston SH, Lobritz MA, Nguyen S, Lassen K, Delair S, Posta F, et al. A quantitative affinity-profiling system that reveals distinct CD4/CCR5 usage patterns among human immunodeficiency virus type 1

- and simian immunodeficiency virus strains. *Journal of virology*. 2009; 83(21):11016–26. Epub 2009/08/21. doi: [10.1128/JVI.01242-09](https://doi.org/10.1128/JVI.01242-09) PMID: [19692480](https://pubmed.ncbi.nlm.nih.gov/19692480/)
92. Salimi H, Roche M, Webb N, Gray LR, Chikere K, Sterjovski J, et al. Macrophage-tropic HIV-1 variants from brain demonstrate alterations in the way gp120 engages both CD4 and CCR5. *Journal of leukocyte biology*. 2013; 93(1):113–26. Epub 2012/10/19. doi: [10.1189/jlb.0612308](https://doi.org/10.1189/jlb.0612308) PMID: [23077246](https://pubmed.ncbi.nlm.nih.gov/23077246/)
 93. Schnell G, Joseph S, Spudich S, Price RW, Swanstrom R. HIV-1 replication in the central nervous system occurs in two distinct cell types. *PLoS pathogens*. 2011; 7(10):e1002286. doi: [10.1371/journal.ppat.1002286](https://doi.org/10.1371/journal.ppat.1002286) PMID: [22007152](https://pubmed.ncbi.nlm.nih.gov/22007152/)
 94. Platt EJ, Wehrly K, Kuhmann SE, Chesebro B, Kabat D. Effects of CCR5 and CD4 cell surface concentrations on infections by macrophagetropic isolates of human immunodeficiency virus type 1. *Journal of virology*. 1998; 72(4):2855–64. Epub 1998/04/03. PMID: [9525605](https://pubmed.ncbi.nlm.nih.gov/9525605/)
 95. Reh L, Magnus C, Schanz M, Weber J, Uhr T, Rusert P, et al. Capacity of Broadly Neutralizing Antibodies to Inhibit HIV-1 Cell-Cell Transmission Is Strain- and Epitope-Dependent. *PLoS pathogens*. 2015; 11(7):e1004966. Epub 2015/07/15. doi: [10.1371/journal.ppat.1004966](https://doi.org/10.1371/journal.ppat.1004966) PMID: [26158270](https://pubmed.ncbi.nlm.nih.gov/26158270/)
 96. Ruprecht CR, Krarup A, Reynell L, Mann AM, Brandenburg OF, Berlinger L, et al. MPER-specific antibodies induce gp120 shedding and irreversibly neutralize HIV-1. *The Journal of experimental medicine*. 2011; 208(3):439–54. Epub 2011/03/02. doi: [10.1084/jem.20101907](https://doi.org/10.1084/jem.20101907) PMID: [21357743](https://pubmed.ncbi.nlm.nih.gov/21357743/)
 97. Zhang S, Alexander L, Wang T, Agler M, Zhou N, Fang H, et al. Protection against HIV-envelope-induced neuronal cell destruction by HIV attachment inhibitors. *Archives of virology*. 2010; 155(5):777–81. Epub 2010/03/20. doi: [10.1007/s00705-010-0644-x](https://doi.org/10.1007/s00705-010-0644-x) PMID: [20300783](https://pubmed.ncbi.nlm.nih.gov/20300783/)
 98. O'Connell O, Repik A, Reeves JD, Gonzalez-Perez MP, Quitadamo B, Anton ED, et al. Efficiency of bridging-sheet recruitment explains HIV-1 R5 envelope glycoprotein sensitivity to soluble CD4 and macrophage tropism. *Journal of virology*. 2013; 87(1):187–98. Epub 2012/10/12. doi: [10.1128/JVI.01834-12](https://doi.org/10.1128/JVI.01834-12) PMID: [23055568](https://pubmed.ncbi.nlm.nih.gov/23055568/)
 99. Sterjovski J, Churchill MJ, Roche M, Ellett A, Farrugia W, Wesselingh SL, et al. CD4-binding site alterations in CCR5-using HIV-1 envelopes influencing gp120-CD4 interactions and fusogenicity. *Virology*. 2011; 410(2):418–28. Epub 2011/01/11. doi: [10.1016/j.virol.2010.12.010](https://doi.org/10.1016/j.virol.2010.12.010) PMID: [21216423](https://pubmed.ncbi.nlm.nih.gov/21216423/)
 100. Stewart-Jones GB, Soto C, Lemmin T, Chuang GY, Druz A, Kong R, et al. Trimeric HIV-1-Env Structures Define Glycan Shields from Clades A, B, and G. *Cell*. 2016; 165(4):813–26. doi: [10.1016/j.cell.2016.04.010](https://doi.org/10.1016/j.cell.2016.04.010) PMID: [27114034](https://pubmed.ncbi.nlm.nih.gov/27114034/)
 101. Schrodinger L. The PyMOL Molecular Graphics System, Version 1.4.1 2015.
 102. Holman AG, Mefford ME, O'Connor N, Gabuzda D. HIVBrainSeqDB: a database of annotated HIV envelope sequences from brain and other anatomical sites. *AIDS research and therapy*. 2010; 7:43. Epub 2010/12/16. doi: [10.1186/1742-6405-7-43](https://doi.org/10.1186/1742-6405-7-43) PMID: [21156070](https://pubmed.ncbi.nlm.nih.gov/21156070/)
 103. Xiang SH, Finzi A, Pacheco B, Alexander K, Yuan W, Rizzuto C, et al. A V3 loop-dependent gp120 element disrupted by CD4 binding stabilizes the human immunodeficiency virus envelope glycoprotein trimer. *Journal of virology*. 2010; 84(7):3147–61. Epub 2010/01/22. doi: [10.1128/JVI.02587-09](https://doi.org/10.1128/JVI.02587-09) PMID: [20089638](https://pubmed.ncbi.nlm.nih.gov/20089638/)
 104. Huang X, Jin W, Hu K, Luo S, Du T, Griffin GE, et al. Highly conserved HIV-1 gp120 glycans proximal to CD4-binding region affect viral infectivity and neutralizing antibody induction. *Virology*. 2012; 423(1):97–106. doi: [10.1016/j.virol.2011.11.023](https://doi.org/10.1016/j.virol.2011.11.023) PMID: [22192629](https://pubmed.ncbi.nlm.nih.gov/22192629/)
 105. Wang W, Nie J, Prochnow C, Truong C, Jia Z, Wang S, et al. A systematic study of the N-glycosylation sites of HIV-1 envelope protein on infectivity and antibody-mediated neutralization. *Retrovirology*. 2013; 10:14. Epub 2013/02/07. doi: [10.1186/1742-4690-10-14](https://doi.org/10.1186/1742-4690-10-14) PMID: [23384254](https://pubmed.ncbi.nlm.nih.gov/23384254/)
 106. Kolchinsky P, Mirzabekov T, Farzan M, Kiprilov E, Cayabyab M, Mooney LJ, et al. Adaptation of a CCR5-using, primary human immunodeficiency virus type 1 isolate for CD4-independent replication. *Journal of virology*. 1999; 73(10):8120–6. Epub 1999/09/11. PMID: [10482561](https://pubmed.ncbi.nlm.nih.gov/10482561/)
 107. Kolchinsky P, Kiprilov E, Bartley P, Rubinstein R, Sodroski J. Loss of a single N-linked glycan allows CD4-independent human immunodeficiency virus type 1 infection by altering the position of the gp120 V1/V2 variable loops. *Journal of virology*. 2001; 75(7):3435–43. Epub 2001/03/10. doi: [10.1128/JVI.75.7.3435-3443.2001](https://doi.org/10.1128/JVI.75.7.3435-3443.2001) PMID: [11238869](https://pubmed.ncbi.nlm.nih.gov/11238869/)
 108. Mefford ME, Gorry PR, Kunstman K, Wolinsky SM, Gabuzda D. Bioinformatic prediction programs underestimate the frequency of CXCR4 usage by R5X4 HIV type 1 in brain and other tissues. *AIDS research and human retroviruses*. 2008; 24(9):1215–20. Epub 2008/09/16. doi: [10.1089/aid.2008.0009](https://doi.org/10.1089/aid.2008.0009) PMID: [18788913](https://pubmed.ncbi.nlm.nih.gov/18788913/)
 109. Byland R, Vance PJ, Hoxie JA, Marsh M. A conserved dileucine motif mediates clathrin and AP-2-dependent endocytosis of the HIV-1 envelope protein. *Mol Biol Cell*. 2007; 18(2):414–25. doi: [10.1091/mbc.E06-06-0535](https://doi.org/10.1091/mbc.E06-06-0535) PMID: [17108326](https://pubmed.ncbi.nlm.nih.gov/17108326/)

110. Mann A, Friedrich N, Krarup A, Weber J, Stiegeler E, Dreier B, et al. Conformation-dependent recognition of HIV gp120 by designed ankyrin repeat proteins provides access to novel HIV entry inhibitors. *Journal of virology*. 2013; 87(10):5868–81. Epub 2013/03/15. doi: [10.1128/JVI.00152-13](https://doi.org/10.1128/JVI.00152-13) PMID: [23487463](https://pubmed.ncbi.nlm.nih.gov/23487463/)
111. Magnus C, Regoes RR. Estimating the stoichiometry of HIV neutralization. *PLoS Comput Biol*. 2010; 6(3):e1000713. doi: [10.1371/journal.pcbi.1000713](https://doi.org/10.1371/journal.pcbi.1000713) PMID: [20333245](https://pubmed.ncbi.nlm.nih.gov/20333245/)
112. Brandenburg OF, Magnus C, Rusert P, Regoes RR, Trkola A. Different infectivity of HIV-1 strains is linked to number of envelope trimers required for entry. *PLoS pathogens*. 2015; 11(1):e1004595. Epub 2015/01/09. doi: [10.1371/journal.ppat.1004595](https://doi.org/10.1371/journal.ppat.1004595) PMID: [25569556](https://pubmed.ncbi.nlm.nih.gov/25569556/)
113. Brandenburg OF, Magnus C, Regoes RR, Trkola A. The HIV-1 Entry Process: A Stoichiometric View. *Trends in microbiology*. 2015; 23(12):763–74. Epub 2015/11/07. doi: [10.1016/j.tim.2015.09.003](https://doi.org/10.1016/j.tim.2015.09.003) PMID: [26541228](https://pubmed.ncbi.nlm.nih.gov/26541228/)
114. Magnus C, Rusert P, Bonhoeffer S, Trkola A, Regoes RR. Estimating the stoichiometry of human immunodeficiency virus entry. *Journal of virology*. 2009; 83(3):1523–31. Epub 2008/11/21. doi: [10.1128/JVI.01764-08](https://doi.org/10.1128/JVI.01764-08) PMID: [19019953](https://pubmed.ncbi.nlm.nih.gov/19019953/)
115. Ping LH, Joseph SB, Anderson JA, Abrahams MR, Salazar-Gonzalez JF, Kincer LP, et al. Comparison of viral Env proteins from acute and chronic infections with subtype C human immunodeficiency virus type 1 identifies differences in glycosylation and CCR5 utilization and suggests a new strategy for immunogen design. *Journal of virology*. 2013; 87(13):7218–33. Epub 2013/04/26. doi: [10.1128/JVI.03577-12](https://doi.org/10.1128/JVI.03577-12) PMID: [23616655](https://pubmed.ncbi.nlm.nih.gov/23616655/)
116. Biancotto A, Iglehart SJ, Vanpouille C, Condack CE, Lisco A, Ruecker E, et al. HIV-1-induced activation of CD4(+) T cells creates new targets for HIV-1 infection in human lymphoid tissue ex vivo. *Blood*. 2008; 111(2):699–704. doi: [10.1182/blood-2007-05-088435](https://doi.org/10.1182/blood-2007-05-088435) PMID: [17909079](https://pubmed.ncbi.nlm.nih.gov/17909079/)
117. Gray L, Roche M, Churchill MJ, Sterjovski J, Ellett A, Pombourios P, et al. Tissue-specific sequence alterations in the human immunodeficiency virus type 1 envelope favoring CCR5 usage contribute to persistence of dual-tropic virus in the brain. *Journal of virology*. 2009; 83(11):5430–41. Epub 2009/03/27. doi: [10.1128/JVI.02648-08](https://doi.org/10.1128/JVI.02648-08) PMID: [19321618](https://pubmed.ncbi.nlm.nih.gov/19321618/)
118. Gorry P, Purcell D, Howard J, McPhee D. Restricted HIV-1 infection of human astrocytes: potential role of nef in the regulation of virus replication. *Journal of neurovirology*. 1998; 4(4):377–86. Epub 1998/08/26. PMID: [9718129](https://pubmed.ncbi.nlm.nih.gov/9718129/)
119. Ellery PJ, Tippett E, Chiu YL, Paukovics G, Cameron PU, Solomon A, et al. The CD16+ monocyte subset is more permissive to infection and preferentially harbors HIV-1 in vivo. *Journal of immunology*. 2007; 178(10):6581–9. Epub 2007/05/04.
120. Verhofstede C, Nijhuis M, Vandekerckhove L. Correlation of coreceptor usage and disease progression. *Current opinion in HIV and AIDS*. 2012; 7(5):432–9. Epub 2012/08/09. doi: [10.1097/COH.0b013e328356f6f2](https://doi.org/10.1097/COH.0b013e328356f6f2) PMID: [22871636](https://pubmed.ncbi.nlm.nih.gov/22871636/)
121. Pollakis G, Paxton WA. Use of (alternative) coreceptors for HIV entry. *Current opinion in HIV and AIDS*. 2012; 7(5):440–9. doi: [10.1097/COH.0b013e328356e9f3](https://doi.org/10.1097/COH.0b013e328356e9f3) PMID: [22842622](https://pubmed.ncbi.nlm.nih.gov/22842622/)
122. Price RW. Neurological complications of HIV infection. *The Lancet*. 1996; 348(9025):445–52.
123. Dunfee RL, Thomas ER, Gabuzda D. Enhanced macrophage tropism of HIV in brain and lymphoid tissues is associated with sensitivity to the broadly neutralizing CD4 binding site antibody b12. *Retrovirology*. 2009; 6:69. Epub 2009/07/22. doi: [10.1186/1742-4690-6-69](https://doi.org/10.1186/1742-4690-6-69) PMID: [19619305](https://pubmed.ncbi.nlm.nih.gov/19619305/)
124. Churchill MJ, Cowley DJ, Wesselingh SL, Gorry PR, Gray LR. HIV-1 transcriptional regulation in the central nervous system and implications for HIV cure research. *Journal of neurovirology*. 2014. Epub 2014/07/26.
125. Arrildt KT, LaBranche CC, Joseph SB, Dukhovlina EN, Graham WD, Ping LH, et al. Phenotypic Correlates of HIV-1 Macrophage Tropism. *Journal of virology*. 2015; 89(22):11294–311. Epub 2015/09/05. doi: [10.1128/JVI.00946-15](https://doi.org/10.1128/JVI.00946-15) PMID: [26339058](https://pubmed.ncbi.nlm.nih.gov/26339058/)
126. Musich T, O'Connell O, Gonzalez-Perez MP, Derdeyn CA, Peters PJ, Clapham PR. HIV-1 non-macrophage-tropic R5 envelope glycoproteins are not more tropic for entry into primary CD4+ T-cells than envelopes highly adapted for macrophages. *Retrovirology*. 2015; 12:25. Epub 2015/03/27. doi: [10.1186/s12977-015-0141-0](https://doi.org/10.1186/s12977-015-0141-0) PMID: [25809903](https://pubmed.ncbi.nlm.nih.gov/25809903/)
127. Mefford ME, Kunstman K, Wolinsky SM, Gabuzda D. Bioinformatic analysis of neurotropic HIV envelope sequences identifies polymorphisms in the gp120 bridging sheet that increase macrophage-tropism through enhanced interactions with CCR5. *Virology*. 2015; 481:210–22. Epub 2015/03/24. doi: [10.1016/j.virol.2015.01.032](https://doi.org/10.1016/j.virol.2015.01.032) PMID: [25797607](https://pubmed.ncbi.nlm.nih.gov/25797607/)
128. Sattentau QJ, Stevenson M. Macrophages and HIV-1: An Unhealthy Constellation. *Cell host & microbe*. 2016; 19(3):304–10. Epub 2016/03/11.

129. Joseph SB, Arrildt KT, Sturdevant CB, Swanstrom R. HIV-1 target cells in the CNS. *Journal of neurovirology*. 2015; 21(3):276–89. Epub 2014/09/23. doi: [10.1007/s13365-014-0287-x](https://doi.org/10.1007/s13365-014-0287-x) PMID: [25236812](https://pubmed.ncbi.nlm.nih.gov/25236812/)
130. Herschhorn A, Ma X, Gu C, Ventura JD, Castillo-Menendez L, Melillo B, et al. Release of gp120 Restraints Leads to an Entry-Competent Intermediate State of the HIV-1 Envelope Glycoproteins. *mBio*. 2016; 7(5). Epub 2016/11/01.
131. Abela IA, Berlinger L, Schanz M, Reynell L, Gunthard HF, Rusert P, et al. Cell-cell transmission enables HIV-1 to evade inhibition by potent CD4bs directed antibodies. *PLoS pathogens*. 2012; 8(4): e1002634. Epub 2012/04/13. doi: [10.1371/journal.ppat.1002634](https://doi.org/10.1371/journal.ppat.1002634) PMID: [22496655](https://pubmed.ncbi.nlm.nih.gov/22496655/)
132. Brandenburg OF, Rusert P, Magnus C, Weber J, Boni J, Gunthard HF, et al. Partial rescue of V1V2 mutant infectivity by HIV-1 cell-cell transmission supports the domain's exceptional capacity for sequence variation. *Retrovirology*. 2014; 11:75. Epub 2014/10/08. doi: [10.1186/s12977-014-0075-y](https://doi.org/10.1186/s12977-014-0075-y) PMID: [25287422](https://pubmed.ncbi.nlm.nih.gov/25287422/)
133. Clavel F, Charneau P. Fusion from without directed by human immunodeficiency virus particles. *Journal of virology*. 1994; 68(2):1179–85. PMID: [8289347](https://pubmed.ncbi.nlm.nih.gov/8289347/)
134. Joseph SB, Swanstrom R, Kashuba AD, Cohen MS. Bottlenecks in HIV-1 transmission: insights from the study of founder viruses. *Nature reviews Microbiology*. 2015; 13(7):414–25. Epub 2015/06/09. doi: [10.1038/nrmicro3471](https://doi.org/10.1038/nrmicro3471) PMID: [26052661](https://pubmed.ncbi.nlm.nih.gov/26052661/)
135. Carlson JM, Schaefer M, Monaco DC, Batorsky R, Claiborne DT, Prince J, et al. HIV transmission. Selection bias at the heterosexual HIV-1 transmission bottleneck. *Science*. 2014; 345(6193):1254031. Epub 2014/07/12. doi: [10.1126/science.1254031](https://doi.org/10.1126/science.1254031) PMID: [25013080](https://pubmed.ncbi.nlm.nih.gov/25013080/)
136. Sturdevant CB, Joseph SB, Schnell G, Price RW, Swanstrom R, Spudich S. Compartmentalized replication of R5 T cell-tropic HIV-1 in the central nervous system early in the course of infection. *PLoS pathogens*. 2015; 11(3):e1004720. doi: [10.1371/journal.ppat.1004720](https://doi.org/10.1371/journal.ppat.1004720) PMID: [25811757](https://pubmed.ncbi.nlm.nih.gov/25811757/)
137. Ivey NS, MacLean AG, Lackner AA. Acquired immunodeficiency syndrome and the blood-brain barrier. *Journal of neurovirology*. 2009; 15(2):111–22. doi: [10.1080/13550280902769764](https://doi.org/10.1080/13550280902769764) PMID: [19306229](https://pubmed.ncbi.nlm.nih.gov/19306229/)
138. Mutnal MB, Hu S, Lokensgard JR. Persistent humoral immune responses in the CNS limit recovery of reactivated murine cytomegalovirus. *PLoS one*. 2012; 7(3):e33143. doi: [10.1371/journal.pone.0033143](https://doi.org/10.1371/journal.pone.0033143) PMID: [22412996](https://pubmed.ncbi.nlm.nih.gov/22412996/)
139. Ousman SS, Kuberski P. Immune surveillance in the central nervous system. *Nat Neurosci*. 2012; 15(8):1096–101. doi: [10.1038/nn.3161](https://doi.org/10.1038/nn.3161) PMID: [22837040](https://pubmed.ncbi.nlm.nih.gov/22837040/)
140. Ransohoff RM, Engelhardt B. The anatomical and cellular basis of immune surveillance in the central nervous system. *Nature reviews Immunology*. 2012; 12(9):623–35. doi: [10.1038/nri3265](https://doi.org/10.1038/nri3265) PMID: [22903150](https://pubmed.ncbi.nlm.nih.gov/22903150/)
141. Bonnan M, Barroso B, Demasles S, Krim E, Marasescu R, Miquel M. Compartmentalized intrathecal immunoglobulin synthesis during HIV infection—a model of chronic CNS inflammation? *J Neuroimmunol*. 2015; 285:41–52. doi: [10.1016/j.jneuroim.2015.05.015](https://doi.org/10.1016/j.jneuroim.2015.05.015) PMID: [26198917](https://pubmed.ncbi.nlm.nih.gov/26198917/)
142. Bruno CJ, Jacobson JM. Ibalizumab: an anti-CD4 monoclonal antibody for the treatment of HIV-1 infection. *The Journal of antimicrobial chemotherapy*. 2010; 65(9):1839–41. doi: [10.1093/jac/dkq261](https://doi.org/10.1093/jac/dkq261) PMID: [20639524](https://pubmed.ncbi.nlm.nih.gov/20639524/)
143. Fessel WJ, Anderson B, Follansbee SE, Winters MA, Lewis ST, Weinheimer SP, et al. The efficacy of an anti-CD4 monoclonal antibody for HIV-1 treatment. *Antiviral research*. 2011; 92(3):484–7. doi: [10.1016/j.antiviral.2011.09.010](https://doi.org/10.1016/j.antiviral.2011.09.010) PMID: [22001594](https://pubmed.ncbi.nlm.nih.gov/22001594/)
144. Schols D, Baba M, Pauwels R, Desmyter J, De Clercq E. Specific interaction of aurantricarboxylic acid with the human immunodeficiency virus/CD4 cell receptor. *Proceedings of the National Academy of Sciences of the United States of America*. 1989; 86(9):3322–6. PMID: [2566170](https://pubmed.ncbi.nlm.nih.gov/2566170/)
145. Pegu A, Yang ZY, Boyington JC, Wu L, Ko SY, Schmidt SD, et al. Neutralizing antibodies to HIV-1 envelope protect more effectively in vivo than those to the CD4 receptor. *Sci Transl Med*. 2014; 6(243):243ra88. Epub 2014/07/06. doi: [10.1126/scitranslmed.3008992](https://doi.org/10.1126/scitranslmed.3008992) PMID: [24990883](https://pubmed.ncbi.nlm.nih.gov/24990883/)
146. Jacobson JM, Israel RJ, Lowy I, Ostrow NA, Vassilatos LS, Barish M, et al. Treatment of advanced human immunodeficiency virus type 1 disease with the viral entry inhibitor PRO 542. *Antimicrob Agents Chemother*. 2004; 48(2):423–9. doi: [10.1128/AAC.48.2.423-429.2004](https://doi.org/10.1128/AAC.48.2.423-429.2004) PMID: [14742190](https://pubmed.ncbi.nlm.nih.gov/14742190/)
147. Jacobson JM, Lowy I, Fletcher CV, O'Neill TJ, Tran DN, Ketas TJ, et al. Single-dose safety, pharmacology, and antiviral activity of the human immunodeficiency virus (HIV) type 1 entry inhibitor PRO 542 in HIV-infected adults. *The Journal of infectious diseases*. 2000; 182(1):326–9. doi: [10.1086/315698](https://doi.org/10.1086/315698) PMID: [10882617](https://pubmed.ncbi.nlm.nih.gov/10882617/)
148. Richard J, Veillette M, Brassard N, Iyer SS, Roger M, Martin L, et al. CD4 mimetics sensitize HIV-1-infected cells to ADCC. *Proceedings of the National Academy of Sciences of the United States of America*. 2015; 112(20):E2687–94. doi: [10.1073/pnas.1506755112](https://doi.org/10.1073/pnas.1506755112) PMID: [25941367](https://pubmed.ncbi.nlm.nih.gov/25941367/)

149. Selhorst P, Grugging K, Tong T, Crooks ET, Martin L, Vanham G, et al. M48U1 CD4 mimetic has a sustained inhibitory effect on cell-associated HIV-1 by attenuating virion infectivity through gp120 shedding. *Retrovirology*. 2013; 10:12. doi: [10.1186/1742-4690-10-12](https://doi.org/10.1186/1742-4690-10-12) PMID: [23375046](https://pubmed.ncbi.nlm.nih.gov/23375046/)
150. Haim H, Si Z, Madani N, Wang L, Courter JR, Princiotta A, et al. Soluble CD4 and CD4-mimetic compounds inhibit HIV-1 infection by induction of a short-lived activated state. *PLoS pathogens*. 2009; 5(4):e1000360. doi: [10.1371/journal.ppat.1000360](https://doi.org/10.1371/journal.ppat.1000360) PMID: [19343205](https://pubmed.ncbi.nlm.nih.gov/19343205/)
151. Stricher F, Huang CC, Descours A, Duquesnoy S, Combes O, Decker JM, et al. Combinatorial optimization of a CD4-mimetic miniprotein and cocrystal structures with HIV-1 gp120 envelope glycoprotein. *Journal of molecular biology*. 2008; 382(2):510–24. doi: [10.1016/j.jmb.2008.06.069](https://doi.org/10.1016/j.jmb.2008.06.069) PMID: [18619974](https://pubmed.ncbi.nlm.nih.gov/18619974/)
152. Gardner MR, Kattenhorn LM, Kondur HR, von Schaeuwen M, Dorfman T, Chiang JJ, et al. AAV-expressed eCD4-Ig provides durable protection from multiple SHIV challenges. *Nature*. 2015; 519(7541):87–91. doi: [10.1038/nature14264](https://doi.org/10.1038/nature14264) PMID: [25707797](https://pubmed.ncbi.nlm.nih.gov/25707797/)
153. Moore JP, Stevenson M. New targets for inhibitors of HIV-1 replication. *Nat Rev Mol Cell Biol*. 2000; 1(1):40–9. doi: [10.1038/35036060](https://doi.org/10.1038/35036060) PMID: [11413488](https://pubmed.ncbi.nlm.nih.gov/11413488/)
154. Klasse PJ, McKeating JA. Soluble CD4 and CD4 immunoglobulin-selected HIV-1 variants: a phenotypic characterization. *AIDS research and human retroviruses*. 1993; 9(7):595–604. doi: [10.1089/aid.1993.9.595](https://doi.org/10.1089/aid.1993.9.595) PMID: [8369164](https://pubmed.ncbi.nlm.nih.gov/8369164/)
155. Lynch RM, Wong P, Tran L, O'Dell S, Nason MC, Li Y, et al. HIV-1 fitness cost associated with escape from the VRC01 class of CD4 binding site neutralizing antibodies. *Journal of virology*. 2015; 89(8):4201–13. Epub 2015/01/30. doi: [10.1128/JVI.03608-14](https://doi.org/10.1128/JVI.03608-14) PMID: [25631091](https://pubmed.ncbi.nlm.nih.gov/25631091/)
156. Rieder P, Joos B, von Wyl V, Kuster H, Grube C, Leemann C, et al. HIV-1 transmission after cessation of early antiretroviral therapy among men having sex with men. *AIDS*. 2010; 24(8):1177–83. Epub 2010/04/14. doi: [10.1097/QAD.0b013e328338e4de](https://doi.org/10.1097/QAD.0b013e328338e4de) PMID: [20386427](https://pubmed.ncbi.nlm.nih.gov/20386427/)
157. Oxenius A, Price DA, Gunthard HF, Dawson SJ, Fagard C, Perrin L, et al. Stimulation of HIV-specific cellular immunity by structured treatment interruption fails to enhance viral control in chronic HIV infection. *Proceedings of the National Academy of Sciences of the United States of America*. 2002; 99(21):13747–52. Epub 2002/10/09. doi: [10.1073/pnas.202372199](https://doi.org/10.1073/pnas.202372199) PMID: [12370434](https://pubmed.ncbi.nlm.nih.gov/12370434/)
158. Oxenius A, McLean AR, Fischer M, Price DA, Dawson SJ, Hafner R, et al. Human immunodeficiency virus-specific CD8(+) T-cell responses do not predict viral growth and clearance rates during structured intermittent antiretroviral therapy. *Journal of virology*. 2002; 76(20):10169–76. Epub 2002/09/20. PMID: [12239291](https://pubmed.ncbi.nlm.nih.gov/12239291/)
159. Fagard C, Oxenius A, Gunthard H, Garcia F, Le Braz M, Mestre G, et al. A prospective trial of structured treatment interruptions in human immunodeficiency virus infection. *Archives of internal medicine*. 2003; 163(10):1220–6. Epub 2003/05/28. doi: [10.1001/archinte.163.10.1220](https://doi.org/10.1001/archinte.163.10.1220) PMID: [12767960](https://pubmed.ncbi.nlm.nih.gov/12767960/)
160. Swiss HIVCS, Schoeni-Affolter F, Ledergerber B, Rickenbach M, Rudin C, Gunthard HF, et al. Cohort profile: the Swiss HIV Cohort study. *International journal of epidemiology*. 2010; 39(5):1179–89. Epub 2009/12/02. doi: [10.1093/ije/dyp321](https://doi.org/10.1093/ije/dyp321) PMID: [19948780](https://pubmed.ncbi.nlm.nih.gov/19948780/)
161. Platt EJ, Madani N, Kozak SL, Kabat D. Infectious properties of human immunodeficiency virus type 1 mutants with distinct affinities for the CD4 receptor. *Journal of virology*. 1997; 71(2):883–90. Epub 1997/02/01. PMID: [8995604](https://pubmed.ncbi.nlm.nih.gov/8995604/)
162. Mann AM, Rusert P, Berlinger L, Kuster H, Gunthard HF, Trkola A. HIV sensitivity to neutralization is determined by target and virus producer cell properties. *AIDS*. 2009; 23(13):1659–67. Epub 2009/07/08. doi: [10.1097/QAD.0b013e32832e9408](https://doi.org/10.1097/QAD.0b013e32832e9408) PMID: [19581791](https://pubmed.ncbi.nlm.nih.gov/19581791/)
163. Rusert P, Mann A, Huber M, von Wyl V, Gunthard HF, Trkola A. Divergent effects of cell environment on HIV entry inhibitor activity. *AIDS*. 2009; 23(11):1319–27. Epub 2009/07/07. PMID: [19579289](https://pubmed.ncbi.nlm.nih.gov/19579289/)
164. Zhong P, Agosto LM, Ilinskaya A, Dorjbal B, Truong R, Derse D, et al. Cell-to-cell transmission can overcome multiple donor and target cell barriers imposed on cell-free HIV. *PloS one*. 2013; 8(1):e53138. Epub 2013/01/12. doi: [10.1371/journal.pone.0053138](https://doi.org/10.1371/journal.pone.0053138) PMID: [23308151](https://pubmed.ncbi.nlm.nih.gov/23308151/)
165. Hamilton JA. Colony-stimulating factors in inflammation and autoimmunity. *Nature reviews Immunology*. 2008; 8(7):533–44. Epub 2008/06/14. doi: [10.1038/nri2356](https://doi.org/10.1038/nri2356) PMID: [18551128](https://pubmed.ncbi.nlm.nih.gov/18551128/)
166. Young DA L L, Clark SC. Comparison of the effects of IL-3, granulocyte-macrophage colony-stimulating factor, and macrophage colony-stimulating factor in supporting monocyte differentiation in culture. Analysis of macrophage antibody-dependent cellular cytotoxicity. *The Journal of Immunology*. 1990; 145(2):607–15. Epub n/a. PMID: [2142182](https://pubmed.ncbi.nlm.nih.gov/2142182/)
167. Vogel DY, Glim JE, Stavenuiter AW, Breur M, Heijnen P, Amor S, et al. Human macrophage polarization in vitro: Maturation and activation methods compared. *Immunobiology*. 2014; 219(9):695–703. Epub 2014/06/12. doi: [10.1016/j.imbio.2014.05.002](https://doi.org/10.1016/j.imbio.2014.05.002) PMID: [24916404](https://pubmed.ncbi.nlm.nih.gov/24916404/)
168. Ambarus CA, Krausz S, van Eijk M, Hamann J, Radstake TR, Reedquist KA, et al. Systematic validation of specific phenotypic markers for in vitro polarized human macrophages. *Journal of*

immunological methods. 2012; 375(1–2):196–206. Epub 2011/11/15. doi: [10.1016/j.jim.2011.10.013](https://doi.org/10.1016/j.jim.2011.10.013) PMID: [22075274](https://pubmed.ncbi.nlm.nih.gov/22075274/)

169. Miyauchi K, Kozlov MM, Melikyan GB. Early steps of HIV-1 fusion define the sensitivity to inhibitory peptides that block 6-helix bundle formation. PLoS pathogens. 2009; 5(9):e1000585. Epub 2009/09/19. doi: [10.1371/journal.ppat.1000585](https://doi.org/10.1371/journal.ppat.1000585) PMID: [19763181](https://pubmed.ncbi.nlm.nih.gov/19763181/)